Temperature Distributional Shocks: Identification and Macroeconomic Effects

Draft in Construction - Please Do Not Circulate It

Maria Dolores Gadea-Rivas[1], Jesús Gonzalo[2], and Andrey Ramos[3]

[1]*Department of Applied Economics at University of Zaragoza, lgadea@unizar.es*
[2]*Department of Economics at Universidad Carlos III de Madrid, jesus.gonzalo@uc3m.es*
[3]*Bank of Spain, andrey.ramos@bde.es*

November 3, 2025

Abstract

This paper introduces a methodology to identify temperature distributional shocks, i.e., shocks capturing shifts not only in the average but also across different quantiles of the temperature process. Using data for the globe and a panel of 21 economies, we consistently recover three types of local and global temperature distributional shocks and estimate their macroeconomic impacts on output growth, total factor productivity, inflation and inequality. The first type of shock captures a classic *distributional shift* and yields economic responses consistent with studies that assume the average temperature as a sufficient statistic for climate change. Our key contribution is to uncover two additional shock-types reshaping the temperature distribution while leaving the average approximately unchanged: (i) a *variability*-shock that moves mid-lower and mid-upper quantiles in opposite directions, and (ii) an *extremes*-shock that shifts the tails relative to the center. These variability and extremes factor-shocks induce economic responses not documented in standard average-based approaches. Our results reveal the value of modeling changes in the whole temperature distribution for climate-macro analysis and carry important implications for social cost of carbon estimation and climate-related risk assessment.

JEL Classification: C32, C50, Q54

Keywords: Temperature Shocks, Economic Damages, Distributional Characteristics, Local Projections, Factor Models

1 Introduction

There is no doubt that climate change is hurting economic activity worldwide. Global average temperature is now more than 1.2°C above pre-industrial levels, and the consequences of this degree of warming are already being felt in the form of more frequent and severe extreme weather events, including droughts, floodings, wildfires, and massive storms (AR6-IPCC, 2021). The climate–economics literature has extensively documented the adverse effects of rising temperatures on economic performance (Dell et al., 2012; Burke et al., 2015; Hsiang et al., 2017; Newell et al., 2021; Neal, 2023; Bilal and Känzig, 2024; Kotz et al., 2024; Nath et al., 2024). The standard empirical approach to estimating climate damages relies on projecting the levels or shocks of local or global average temperatures onto economic outcomes using panel or time-series methods (Hassler et al., 2024; Bilal and Stock, 2025). This strategy implicitly assumes that the mean temperature is a sufficient statistic for climate change effectively capturing all climatic forces that influence economic activity.

However, under the well-established heterogeneity in climate change dynamics across space and time (Chapman et al., 2013; Ji et al., 2014; Gadea and Gonzalo, 2025), assuming the average temperature as a sufficient statistic for climate change may yield biased estimates of true economic damages: projecting only averages masks the potential effects of changes in other characteristics of the temperature distribution that may exert distinct and non-linear effects on economic outcomes. This paper addresses this limitation by proposing a new methodology to identify *temperature distributional shocks*, i.e., shocks that capture not only shifts in the mean but also across different quantiles of the temperature process. The identification strategy proceeds in three steps. First, annual time series of temperature distributional characteristics are constructed following Gadea and Gonzalo (2020) using data from Version 4 of the Climatic Research Unit gridded Time Series (CRU–TS v4) dataset (Harris et al., 2020). Second, individual shocks are extracted by applying the Hamilton (2018) filter to each individual characteristic,[1] isolating deviations from their long-run trends. Third, because the resulting shocks are contemporaneously correlated, a factor model (Bai and Ng, 2002) is employed to extract a small number of uncorrelated latent factors summarizing their common sources of variation.

The empirical analysis distinguishes between global and local temperature distributional shocks. Global characteristics are computed from the annual cross-sectional distribution of all temperature grids worldwide, whereas local characteristics are derived from country-specific subsets of these

[1] This extends the procedure in Bilal and Känzig (2024) from average temperature shocks to the full temperature distribution.

grids. In both cases, the factor decomposition of the matrices of Hamilton-filtered shocks consistently identifies three orthogonal common factors capturing the dominant sources of co-movement across distributional characteristics. The first factor corresponds to a classic *distributional shift*, with same-sing loadings across all characteristics, and representing innovations that shift the entire temperature distribution in the same direction as the average. The second factor, characterized by loadings of opposite sign in the lower and upper parts of the distribution, reflects changes in *variability*, i.e., widening or narrowing of the temperature range around the mean. The third factor displays positive loadings in both tails and negative loadings at central quantiles, capturing *extremes* shocks associated with an intensification of temperature extremes relative to median conditions.

The dynamic macroeconomic effects of these shocks on output growth, total factor productivity (TFP), inflation, and inequality are estimated using country-level local projections (Jordà, 2005). We consider a sample of 21 countries for which we have reliable economic data. A brief summary of the results is as follows. Responses of output and TFP to the local and global *distributional shift* factor are aligned to the standard literature documenting contractionary effects of mean-temperature shocks. Once higher-order temperature shocks are considered, additional dimensions of climate risk emerge. While in the United States the *distributional shift* factor alone is sufficient to explain output responses, in other economies—such as France and Switzerland—the *variability* and *extremes* local factors generate additional and persistent output and TFP declines. In Spain, the *extremes* local factor is an important source of output losses while the *distributional shift* factor has no effect. These type of findings cannot be uncovered in analyses restricted to mean temperature and reveal the value of accounting for changes in the entire temperature distribution when assessing the macroeconomic impacts of climate change.

The motivation for distinguishing between global and local temperature distributional shocks lies in their fundamentally different propagation mechanisms, as illustrated in Figure 1. Global shocks represent innovations to the worldwide temperature distribution that originate from large-scale physical forcings—such as variations in the Earth's radiative balance, changes in greenhouse gas concentrations, volcanic aerosols, or ocean–atmosphere cycles like ENSO—which jointly modify the global mean and the shape of the temperature distribution (Hansen et al., 2005; Trenberth et al., 2014). These shocks affect all regions simultaneously, both directly through higher average temperatures and indirectly through the intensification of extreme events (Bilal and Känzig, 2024; AR6-IPCC, 2021), disruptions in trade networks (Neal, 2023), and shifts in world energy and food markets. By contrast, local shocks capture country-specific innovations in the temperature distribution arising from regional circulation anomalies, land–atmosphere feedbacks, or topographical heterogeneity (Quesada et al., 2012; Screen and Simmonds, 2014; Brunner et al., 2017). Their

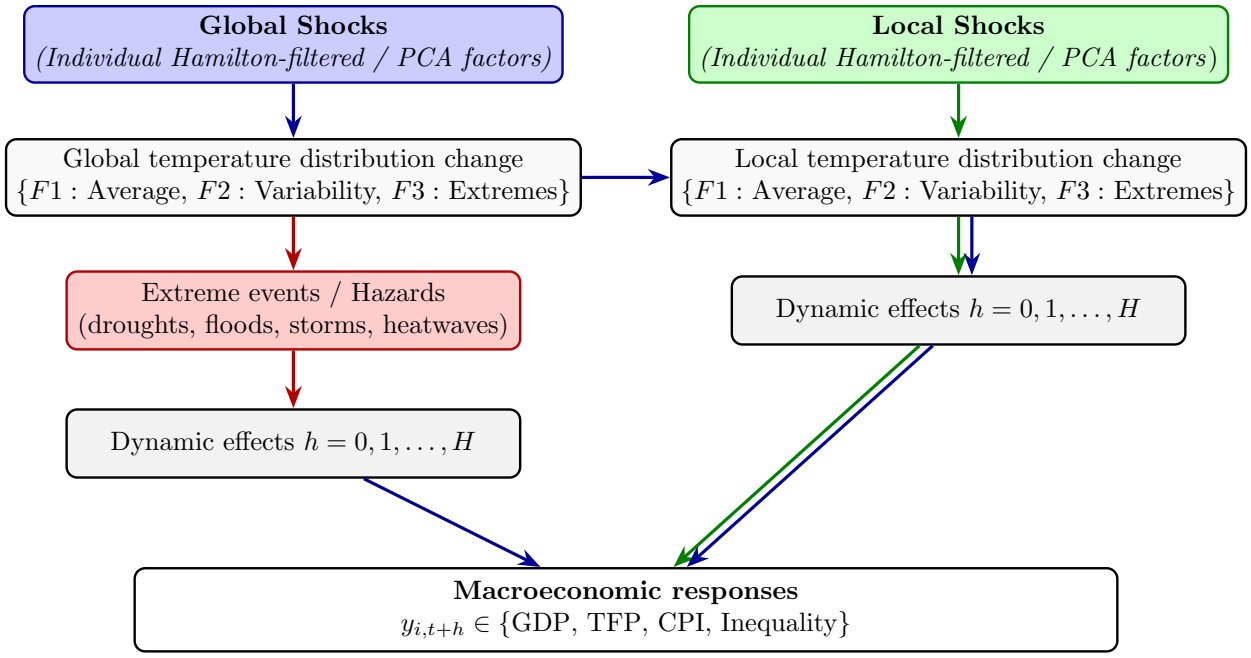


Figure 1: Transmission mechanisms of global and local temperature shocks

macroeconomic transmission operates primarily through domestic production, labor productivity, and price channels, and their effects may differ markedly from global shocks in persistence, sign, and magnitude. Together, these two dimensions generate distinct yet interconnected pathways through which climate variability influences economic activity: global factors shaping the common climate baseline and local factors mediating region-specific responses.

Understanding the macroeconomic consequences of climate change is fundamental for designing effective adaptation and mitigation policies. Reduced-form damage estimates combined with growth models are routinely used to compute welfare losses and to calibrate the Social Cost of Carbon (SCC) (Bilal and Stock, 2025). Recent estimates by Bilal and Känzig (2024) place the SCC at \$1,367 per ton of CO_2, among the highest reported in the literature. In the presence of additional shocks to the temperature distribution not captured by the mean, the true SCC is likely even higher. Our results therefore underscore the need to incorporate temporal and spatial heterogeneity in climate dynamics into damage assessments to capture the full range of climate-related economic consequences.

This paper extends the recent contributions of Bilal and Känzig (2024) and Nath et al. (2024) beyond the average temperature, providing a unified empirical framework to study macroeconomic responses to shocks across the entire global and local temperature distributions. Related studies—such as Colacito et al. (2019), Cipollini et al. (2023), and Nguyen (2024)—examine seasonal

or within-year variations in temperature, while others focus on shocks to specific moments such as variability, skewness, or kurtosis (Donadelli et al., 2022; Kotz et al., 2021; Giraldo et al., 2025). To the best of our knowledge, this paper is the first to analyze individual shocks to temperature distributional characteristics and to extract their uncorrelated sources of common variation using a factor model. The finding that co-movements in these shocks are driven by three distinct factors constitutes a novel empirical result in the climate–economics literature.

The remainder of the paper is organized as follows. Section 2 reviews the related literature. Section 3 describes the data and methodology. Section 4 presents the empirical results and robustness analyses. Section 5 concludes.

2 Related Literature

This paper contributes to the expanding literature that quantifies the economic effects of climate change. Existing studies can broadly be classified into two approaches: *bottom-up* semi-structural models and *top-down* reduced-form analyses (Hsiang, 2016; Hassler et al., 2024). Recent surveys by Lemoine et al. (2025) and Kopits et al. (2025) provide comprehensive overviews of both traditions.

Bottom-up approaches specify explicit mechanisms linking climate change and economic outcomes—such as agricultural yields, labor productivity, or health—and then aggregate sectoral damages using semi-structural models. Classic contributions include the early integrated assessment models of Nordhaus (1992) and Tol (2002). Subsequent work, such as the European Commission's PESETA ((Projection of Economic Impacts of Climate Change in Sectors of the European Union Based on boTtom-up Analysis) project, has refined these analyses for Europe and the United Kingdom, producing detailed assessments of physical and sectoral damages. For instance, the PESETA IV report (Feyen et al., 2020) estimates that a global warming of three degrees would reduce welfare in the European Union by roughly 1.38% percent of GDP per year. While bottom-up estimates are informative about mechanisms, they are often incomplete, as not all climate–economy linkages can be explicitly modeled, and they depend heavily on modeling/calibration choices.

This paper belongs to the second group of studies, *top-down*, an approach that exploits observed historical variation in climate variables to estimate their aggregate economic effects. The canonical specification relates GDP growth or levels to average temperature and precipitation in panel data with fixed effects models, so that identification relies on year-to-year idiosyncratic weather fluctuations. The pioneering work of Dell et al. (2012) showed that a 1°C increase in temperature reduces annual GDP growth by roughly 1.3% in poor countries but has negligible effects in rich ones. Burke

et al. (2015) extended this framework by demonstrating a nonlinear, concave relationship between productivity and temperature, with a global optimum near 13°C. Subsequent studies—including Burke et al. (2018), Kahn et al. (2021), Kotz et al. (2021), and Newell et al. (2021)—confirmed the robustness of these relationships and documented medium-term output losses of between 0.5 and 2.0% of GDP.

Despite their empirical success, these panel models face several econometric challenges. Nath et al. (2024) emphasize three: *i)* including lags of temperature and GDP is crucial to mitigate biases and prevents incorrect inferences about growth versus level effects, *ii)* nonlinearities are better modeled through state dependence than through quadratic terms; and *iii)* causal inference should rely on innovations (temperature shocks) rather than on the levels of temperature itself. Building on these insights, Nath et al. (2024) define temperature shocks as innovations to a nonlinear autoregressive temperature process and estimate their macroeconomic effects using state-dependent local projections (Gonçalves et al., 2024). The resulting impulse responses reveal large and persistent GDP growth losses, consistent with the high temporal persistence of temperature shocks.

A key assumption in most of these studies is that a country's economic outcomes respond only to its own local temperature, while global temperature dynamics or the shocks of trading partners and neighbors are treated as exogenous or part of the error term. Recent work has questioned this assumption. Neal (2023), for example, shows that augmenting traditional growth regressions with global average temperature—following the logic of Dell et al. (2012) and Burke et al. (2015)—substantially changes both the magnitude and interpretation of estimated damages: once global temperature is controlled for, local temperature shocks capture relative, not absolute, climate variation, and estimated damages become markedly larger. Along similar lines, Bilal and Känzig (2024) use time-series methods to isolate both local and global temperature shocks following the procedure of Hamilton (2018). Using local projections, they find that a 1°C global temperature shock reduces cumulative world GDP growth by about 12% at its peaking (six years after the shocks)—roughly six times larger than the estimates from panel regressions based solely on local fluctuations. The difference arises because panel fixed effects implicitly remove the common component of temperature variation, masking the global temperature contribution. Global temperature shocks are often associated with large-scale extreme events such as droughts, extreme winds, and heavy precipitation, which tend to have more pronounced effects on economic activity.

While economic growth is by far the most studied outcome, the macroeconomic effects of climate change extend to other domains. Recent work has examined prices and inflation (Faccia et al., 2021; Ciccarelli and Marotta, 2024; Kotz et al., 2024; Lucidi et al., 2024), inequality (Gilli et al., 2024;

Mumtaz and Theophilopoulou, 2024), and fiscal or financial risks (Zenios, 2022; Barrage, 2024; Pintus et al., 2024; Akyapı et al., 2025). Most studies focus exclusively on the effects of changes in local or global average temperatures implicitly assuming that the average is a sufficient statistic for climate change. A growing set of contributions challenges this assumption. Colacito et al. (2019), Nguyen (2024), and Cipollini et al. (2023), for example, move beyond annual averages by exploiting seasonal temperature variation. Nguyen (2024) finds that warmer winters temporarily boost employment growth in U.S. counties, whereas hotter summers lead to persistent losses. Another closely related strand focuses on the effects of climate volatility and higher-moment risks. Alessandri and Mumtaz (2025) study temperature risk, defined as volatility in average shocks within a VAR with stochastic volatility, linking greater climate uncertainty to lower expected growth. Donadelli et al. (2022) instead consider a different concept of volatility and construct a measure of within-year temperature variability with contractionary effects on productivity growth. Giraldo et al. (2025) extend this logic by modeling variance, skewness, and kurtosis of temperature distributions and analyze their effects on the conditional distribution of GDP growth.

Our work is closest to the latter studies but differs in both scope and methodology. Specifically, we introduce a novel framework that extends the recent average-shock-based approaches of Bilal and Känzig (2024) or Nath et al. (2024) to a broader set of temperature distributional characteristics. Compared to Donadelli et al. (2022) and Giraldo et al. (2025), we do not impose the nature of the shock by simply introducing higher moments characteristics as regressors: our shocks are data-driven, derived from observed temperature characteristics dynamics. The resulting three-factor structure—capturing shifts in the distribution's location, spread, and extremes, provides an empirical representation of climate variability that, to our knowledge, has not been previously documented in the climate-economics literature. This framework reveals macroeconomic responses that cannot be uncovered by analyses focusing solely on average temperature shocks.

3 Methodology

3.1 Data

Temperature data is obtained from Version 4 of the Climatic Research Unit gridded Time Series (CRU–TS v4) dataset (Harris et al., 2020). CRU–TS v4 reports monthly average temperatures for land grid cells (excluding Antarctica) at $0.5° \times 0.5°$ spatial resolution. Data for 67,420 grids from 1901 to 2023 is available, with no missing observations. Macroeconomic variables include real GDP per capita, total factor productivity (TFP), consumer price inflation, and income inequality. Table 1

lists data sources and series definitions. The empirical analysis is conducted at annual frequency over 1960–2019, the longest span with broad coverage across macroeconomic series. The country sample comprises the 21 the OECD economies mentioned in Table 2, although the methodology is applicable to any region or country for which gridded temperatures and macro data are available. For expositional clarity, figures in the main text focus on a subset of eight countries, while results for the full sample are reported in the Online Appendix.

Table 1: Data Description and Sources

Variable	Description	Starting	Source
Output	GDP per capita in constant 2015 US dollars	1960	World Development Indicators (World Bank)
Prices	Consumer Price Index (2010 = 100)	1960	World Development Indicators (World Bank)
TFP	Total Factor Productivity, 2010 U.S. Dollars	1960	Bergeaud et al. (2016)
Inequality	Palma ratio pre-tax	1960	World Inequality Database
Temperature	Gridded Temperature in ∘C	1901	Climatic Research Unit (CRU)

Table 2: List of Countries and ISO3 Codes

Country	ISO3	Country	ISO3	Country	ISO3
Australia	AUS	Austria	AUT	Belgium	BEL
Canada	CAN	Switzerland	CHE	Chile	CHL
Germany	DEU	Denmark	DNK	Spain	ESP
Finland	FIN	France	FRA	United Kingdom	GBR
Greece	GRC	Ireland	IRL	Italy	ITA
Japan	JPN	Mexico	MEX	Norway	NOR
Portugal	PRT	Sweden	SWE	United States	USA

Notes: ISO3 codes follow the ISO 3166–1 alpha–3 standard. The sample includes OECD economies with consistent temperature and macroeconomic data for 1960–2019.

3.2 Temperature Distributional Characteristics

Temperature distributional characteristics are obtained following the approach in Gadea and Gonzalo (2020) and Gadea and Gonzalo (2025). Specifically, temperature is treated as a functional stochastic process denoted by $T = (T_t(\omega), t \in \mathcal{T})$, where $\mathcal{T}$ is an interval in $\mathbb{R}$, defined on a probability space $(\Omega, \mathcal{F}, P)$. For each realization $\omega \in \Omega$, the mapping $t \mapsto T_t(\omega)$ belongs to a function space $\mathbf{G}$, equipped with an inner product, norm, and Borel σ-algebra $\mathcal{B}_G$. In modeling the temperature process T_t, one can either consider the entire sequence of functional objects in $\mathbf{G}$—such as the time series of state densities $\{f_t(\omega)\}_{t=1}^{T}$—or focus on a finite set of *distributional characteristics* $\{C_t^j(\omega)\}_{j=1}^{J}$ summarizing the key features of T_t.

This paper adopts the latter approach. Assume that at each period t and for any spatial domain

i (the globe or a given country) we observe a sufficiently large cross-section of temperature grids, indexed by $n = 1, \ldots, N$. Under standard regularity conditions (see Gadea and Gonzalo, 2020 for mathematical details), we can consistently estimate the vector of unconditional distributional characteristics $Z_{it} = \left[\bar{T}_{it},\ Q_{it}(0.05),\ Q_{it}(0.10),\ \ldots,\ Q_{it}(0.95)\right]'$, where $\bar{T}_{it}$ is the cross-sectional mean temperature, and $Q_{it}(\tau)$ denotes the unconditional τ–quantile of the temperature distribution. These characteristics summarize the entire cross-sectional temperature distribution and form the basis of our empirical analysis. Each element of Z_{it} constitutes a time-series object, which enables the use of conventional econometric methods for filtering, inference, and forecasting.

3.3 Identification of Distributional Temperature Shocks

Let Z_{it} denote the vector of temperature distributional characteristic for country i at time t, obtained using the set of CRU–TS v4 grids covering all land areas within that country. Z_{it}^{j} is the j-th element of Z_{it}. Building on recent work examining the macroeconomic effects of climate change, we focus on the impact of *temperature shocks* rather than temperature levels. Temperature shocks in our baseline analysis are defined as deviations of temperature characteristics from their long-run trends and are extracted by applying the Hamilton (2018) filter separately to each distributional characteristic Z_{it}^{j}. This approach generalizes the analysis of Bilal and Känzig (2024) beyond the mean to other parts of the temperature distribution.

Formally, for each characteristic Z_{it}^{j}, the Hamilton filter is implemented through the regression:

$$Z_{it+h}^{j} = \alpha_{ih}^{j} + \beta_{i0}^{j} Z_{it}^{j} + \beta_{i1}^{j} Z_{it-1}^{j} + \cdots + \beta_{ip}^{j} Z_{it-p+1}^{j} + u_{it+h}^{j}, \tag{1}$$

where u_{it+h}^{j} represents the innovation to the process. The estimated residuals,

$$S_{it+h}^{j} = Z_{it+h}^{j} - \left(\hat{\alpha}_{ih}^{j} + \sum_{k=0}^{p-1} \hat{\beta}_{ik}^{j} Z_{it-k}^{j} \right), \tag{2}$$

define the individual *local temperature distributional shocks*. Global temperature shocks are obtained analogously by applying Equation (1) to characteristics using gridded data for the whole globe. Temperature distributional shocks, either local or global, capture the unpredictable component of each temperature characteristic, orthogonal to its long-run dynamics. In the baseline specification, we set $h = 2$ and $p = 2$, following the standard implementation in Bilal and Känzig (2024). This implies that shocks represent two-year-ahead innovations in temperature that are uncorrelated with the preceding two years of observations. Our results are robust to alternative

choices of (h, p) and to alternative procedures to obtain shocks.

Exogeneity considerations. Identification of causal effects relies on the assumption that temperature shocks provide an exogenous source of variation with respect to economic outcomes. Two arguments support this condition. First, as emphasized by Bilal and Känzig (2024), short-term deviations of temperature from its trend are primarily driven by external forcings—such as volcanic eruptions, solar cycles, and stratospheric aerosol variations—or by internal climate variability, including El Niño and La Niña episodes. These phenomena are determined by physical processes unrelated to contemporaneous macroeconomic activity. The probability that economic conditions could influence such sources of climate variability over a one- to two-year horizon is negligible. Second, the reverse channel from economic activity to temperature is also empirically limited in the short run. According to Carleton et al. (2022), only about 10–20% of the temperature response to a CO_2 emission pulse materializes within the first year, implying that short-term fluctuations in output or emissions have a minimal impact on temperature. Consequently, our Hamilton-filtered shocks can be interpreted as *quasi-exogenous innovations* to the temperature distribution, suitable for causal inference in subsequent macroeconomic analyses.

3.4 A Factor Model for Temperature Distributional Shocks

Individual temperature distributional shocks are inherently correlated. A shock to the average or to a specific quantile often originates from a common physical driver that simultaneously affects other parts of the temperature distribution. This pattern has been documented, for example, by Cipollini et al. (2023) for seasonal temperature shocks in Europe. A natural way to address this correlation is to orthogonalize shocks by imposing an ordering of the distributional characteristics and performing a Cholesky-type decomposition. However, in the absence of strong prior knowledge on such an ordering, this approach can complicate interpretation and limit comparability across countries. Instead, we summarize the common variation in the individual shocks through a factor structure.

Formally, let S_{it} denote the J-dimensional vector collecting the Hamilton-filtered shocks to the J temperature distributional characteristics for geographical unit i. We assume that S_{it} admits the approximate static factor representation (Bai and Ng, 2002, 2013):

$$S_{it} = \Lambda_i f_{it} + \varepsilon_{it}, \tag{3}$$

where f_{it} is an $(r \times 1)$ vector of latent common factors capturing systematic sources of variation

among shocks, Λ_i is the $(J \times r)$ matrix of factor loadings linking each temperature characteristic to the common shocks, and ε_{it} is a $(J \times 1)$ vector of idiosyncratic components, possibly weakly correlated over time and across characteristics. Equation (3) provides a compact representation of the high-dimensional system of shocks, allowing a few latent factors to summarize the dominant modes of co-movement in S_{it}.

The factor model in Equation (3) is not identified without additional restrictions. For any non-singular $r \times r$ matrix H, the transformation $f_{it}^* = Hf_{it}$ and $\Lambda_i^* = \Lambda_i H^{-1}$ yields the same model for S_{it}. To achieve identification (up to sign and permutation), we follow the standard normalization $\frac{1}{T} f_{it}' f_{it} = I_r$ and assume that $\Lambda_i' \Lambda_i$ is diagonal (Bai and Ng, 2013; Stock and Watson, 2016). Under these conventions, the factors and loadings are uniquely defined up to column sign. Estimation proceeds by principal-components solution Bai and Ng (2002). The number of common factors r is selected using a combination of empirical diagnostics: (i) the scree plot of eigenvalues, (ii) the eigenvalue ratio statistic of Ahn and Horenstein (2013), and (iii) the information criteria of Alessi et al. (2010). This approach ensures a parsimonious yet data-driven decomposition of global and local temperature shocks into their principal modes of variation.

3.5 Macroeconomic Effects of Temperature Distributional Shocks

The macroeconomic effects of global and local temperature distributional shocks are estimated using local projections (LPs) (Jordà, 2005)). Let $y_{i,t}$ denote the macroeconomic variable of interest for unit i, such as (log) real GDP per capita, (log) total factor productivity (TFP), (log) consumer price index, or inequality. Following Jordà and Taylor (2024), we estimate cumulative-type LPs taking the form:

$$y_{it+h} - y_{it-1} = \alpha_{ih} + \theta_{ih} w_{it} + \mathbf{x}_{it}' \gamma_{ih} + \varepsilon_{it+h}, \tag{4}$$

for horizons $h = 0, 1, \ldots, H$ and for each i.[2] The term w_{it} denotes the temperature shock—either the individual Hamilton-filtered characteristic or one of the estimated factor shocks—and $\mathbf{x}_{it}$ includes global and region-specific controls, such as lagged values ofw_{it} and of Δy_{it}, to account for persistence and serial correlation. The coefficient θ_{ih} measures the effect of a one-unit temperature shock on the cumulative change of y_{it} at horizon h.[3] Estimation proceeds separately for each horizon h and region i, yielding the sequence $\{\hat{\theta}_{il}\}_{l=0}^{H}$, which forms the impulse response function

[2]The analysis is at the time-series level for each country at the time. We do not employ panel data methods.
[3]Results are robust to the use of a level-type LP regression.

(IRF). Confidence intervals are computed via heteroskedasticity- and autocorrelation-robust block bootstrap procedures.

For joint inference across horizons, we stack the LP equations across horizons into a block-diagonal system:

$$\underbrace{\begin{bmatrix} y_t^{(0)} \\ y_t^{(1)} \\ \vdots \\ y_t^{(H)} \end{bmatrix}}_{\mathbf{y}_{\text{stacked}}} = \underbrace{\begin{bmatrix} \mathbf{X}_0 & 0 & \cdots & 0 \\ 0 & \mathbf{X}_1 & \cdots & 0 \\ \vdots & & \ddots & \vdots \\ 0 & 0 & \cdots & \mathbf{X}_H \end{bmatrix}}_{\mathbf{X}_{\text{block}}} \underbrace{\begin{bmatrix} \hat{\boldsymbol{\theta}}_0 \\ \hat{\boldsymbol{\theta}}_1 \\ \vdots \\ \hat{\boldsymbol{\theta}}_H \end{bmatrix}}_{\hat{\boldsymbol{\theta}}_{\text{stacked}}} + \underbrace{\begin{bmatrix} \hat{u}_t^{(0)} \\ \hat{u}_t^{(1)} \\ \vdots \\ \hat{u}_t^{(H)} \end{bmatrix}}_{\hat{\mathbf{u}}_{\text{stacked}}}. \tag{5}$$

where each block $\mathbf{X}_h$ contains regressors for horizon h, and $\hat{\boldsymbol{\theta}}_{\text{stacked}}$ stacks the estimated coefficients $\hat{\theta}_h$ for all horizons. Let $\mathbf{B}$ be a selection matrix that isolates the coefficients on S_t across horizons:

$$\hat{\boldsymbol{\theta}_h} = \mathbf{B}\,\hat{\boldsymbol{\theta}}_{\text{stacked}}. \tag{6}$$

Wald statistics for the joint significance of responses across all horizons ($H_0: \ \theta_h = 0$ for all h vs. $H_1 : \theta_h \neq 0.$ for some h) are obtained using:

$$W_{\text{joint}} = \hat{\boldsymbol{\theta}}' \left(\mathbf{B}\, \widehat{\text{Var}}(\hat{\boldsymbol{\theta}}_{\text{stacked}})\, \mathbf{B}' \right)^{-1} \hat{\boldsymbol{\theta}} \sim \chi^2_{H+1}, \tag{7}$$

whereas the cumulative significance (sum of responses) is tested ($H_0: \ \sum_h \theta_h = 0$ vs. $H_1: \ \sum_h \theta_h \neq 0.$) following:

$$W_{\text{sum}} = \frac{(\mathbf{1}'\hat{\boldsymbol{\theta}})^2}{\mathbf{1}'\, \widehat{\text{Var}}(\hat{\boldsymbol{\theta}}_{\text{stacked}})\, \mathbf{1}} \sim \chi^2_1, \tag{8}$$

where $\mathbf{1}$ is a vector of ones. These statistics provide joint inference on the dynamic causal effects of temperature shocks across horizons and are reported in all empirical figures.

The whole methodological workflow is summarized in Figure 2.

4 Results

This section is organized in three parts. The first part focuses on the identification of local and global temperature distributional shocks. The second part quantifies the dynamic causal effects of these shocks on output growth, total factor productivity, consumer prices, and income inequality.

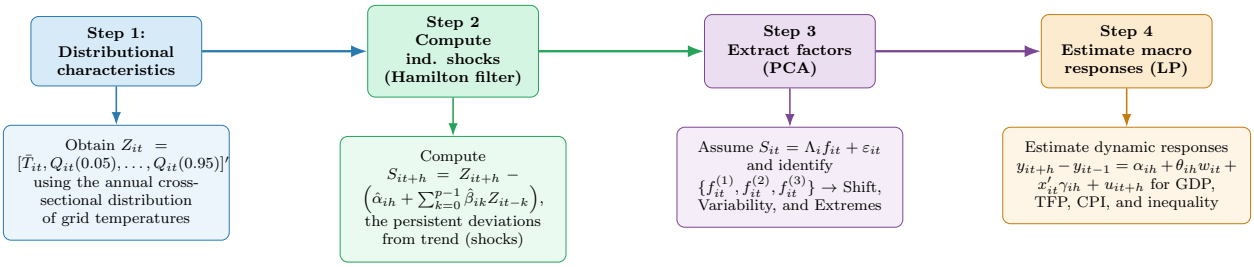


Figure 2: Methodological workflow

The third part assesses the robustness of our results to alternative design choices. The empirical analysis focuses on a set of eight selected countries: the United States (USA), Germany (DEU), France (FRA), Spain (ESP), Switzerland (CHE), Norway (NOR), Mexico (MEX), and Chile (CHL). These countries are chosen to provide coverage across advanced and emerging economies, as well as across climatic zones ranging from temperate to tropical and polar regions. A summary of the joint and cumulative (sum) significance tests for output and productivity responses across the full set of countries is reported in Tables A1 and A2 in the Appendix. Detailed country-specific impulse response figures are provided in the Online Appendix.

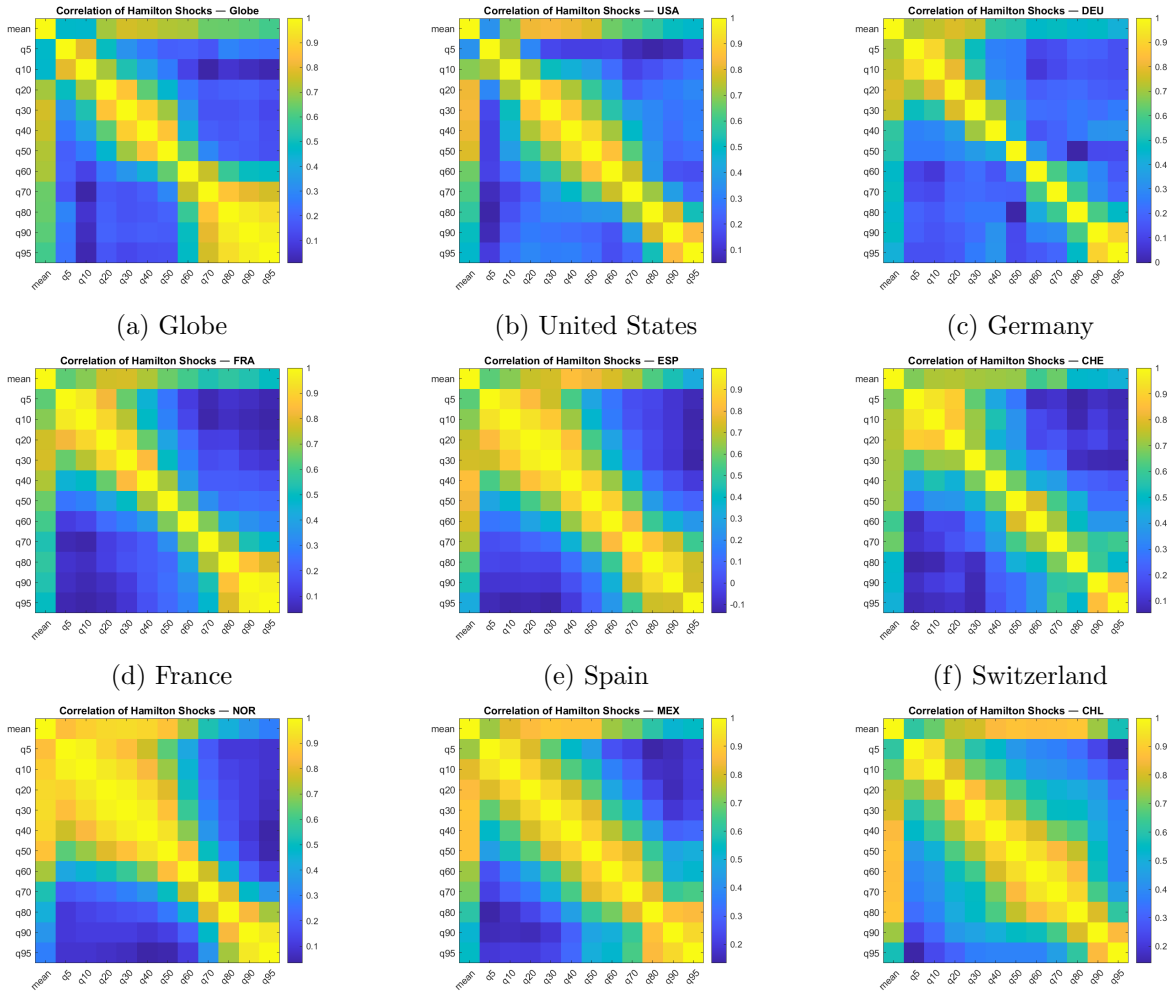
4.1 Identification of Global and Local Temperature Distributional Shocks

Let $Z_{it} = \left[\bar{T}_{it},\ Q_{it}(0.05),\ Q_{it}(0.10),\ \ldots,\ Q_{it}(0.95)\right]'$ be the vector collecting the distributional characteristics of temperature for unit i at time t, where i denotes either the globe or an individual country in our sample. Z_{it} contains the average temperature, $\bar{T}_{it}$, and a set of eleven selected quantile curves $Q_{it}(\tau)$ ranging from $\tau = 0.05$ to $\tau = 0.95$.[4] Shocks to each characteristic are obtained by applying the Hamilton (2018) filter to the corresponding time series.[5] The resulting vector of individual distributional shocks is denoted by S_{it}.

Correlation among shocks. Figure 3 presents the contemporaneous correlation matrices among the elements of S_{it} for both the globe and the set of selected countries. Shocks to different parts of the temperature distribution are correlated and the structure of this correlation vary across geographical areas. In all cases, shocks to the average temperature are strongly correlated with shocks to specific quantiles, while a higher degree of co-movement is observed for adjacent quantiles. For the globe (panel [a]), a pronounced correlation cluster emerges among the upper quantiles. This is not the case of Norway (panel [g]) where the correlation structure is stronger in the lower quantiles.

[4] The analysis is robust to the inclusion of different numbers of quantiles or alternative spacing of τ.
[5] The analysis in Bilal and Känzig (2024) is a particular case of our framework when $Z_{it} = \bar{T}_{it}$.

The contemporaneous correlation across individual temperature distributional shocks reflects the presence of global and regional mechanisms that jointly influence multiple dimensions of the temperature distribution. For example, changes in the Earth's net radiative balance constitute a fundamental forcing that affects all distributional characteristics. Large-scale modes of variability such as the El Niño–Southern Oscillation (ENSO), volcanic aerosols, and fluctuations in solar irradiance are well-known to generate shifts in both the mean and the higher moments of temperature (e.g., Hansen et al., 2005; Trenberth et al., 2014; Knutti and Rugenstein, 2015). These physical drivers alter not only the central tendency of temperature but also its dispersion, skewness, and tail behavior, producing correlated innovations across quantiles.



(a) Globe (b) United States (c) Germany

(d) France (e) Spain (f) Switzerland

(g) Norway (h) Mexico (i) Chile

Figure 3: Correlation plots of individual shocks

Factor analysis. The empirical correlation structure observed in Figure 3 motivates the use of a factor model (Bai and Ng, 2002, 2013) to summarize the common dynamics in the shock

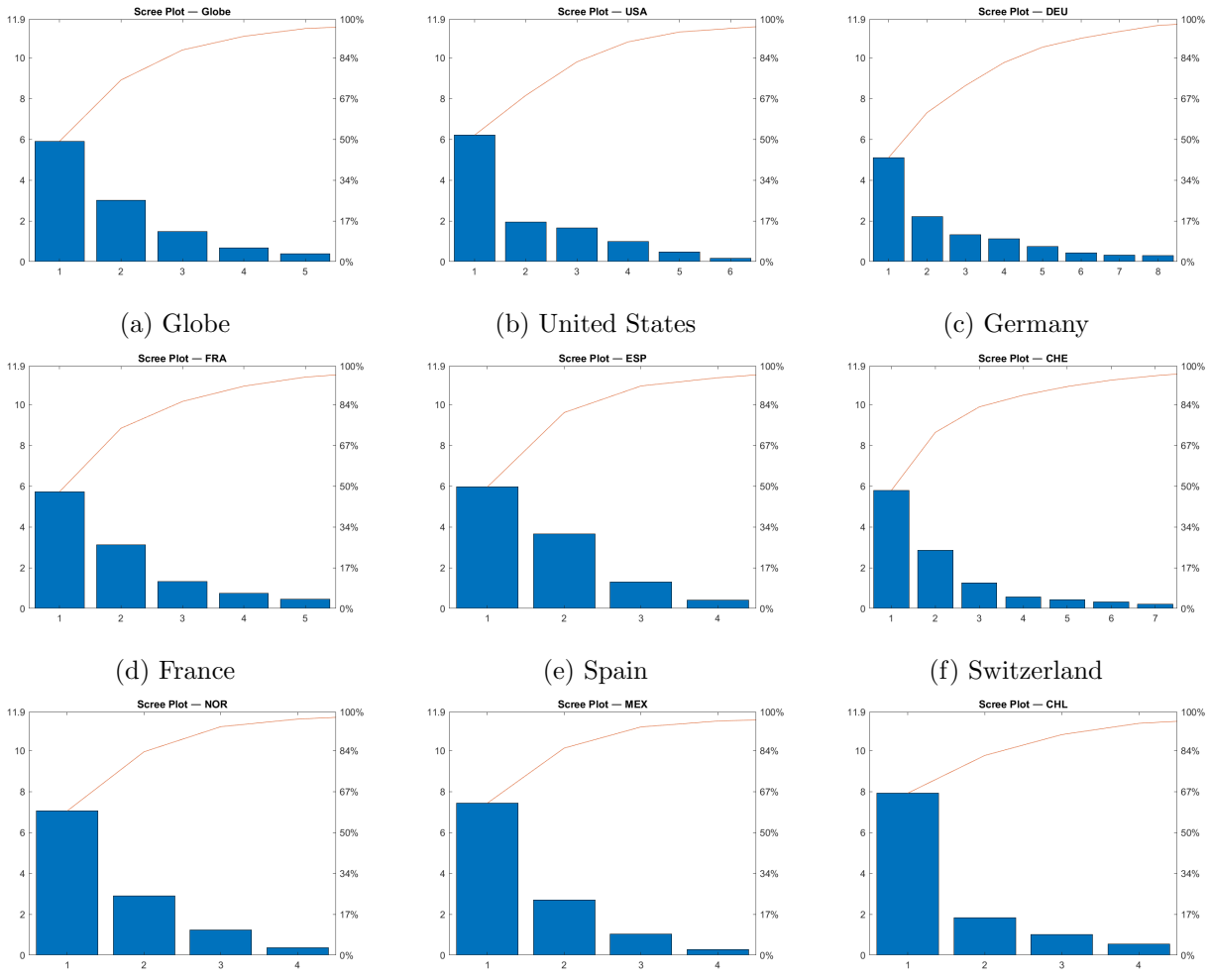
matrices through a small set of latent factors estimated via principal components (PC).[6] The PC factors are linear combinations of the original shock series that are mutually orthogonal by construction, thereby delivering contemporaneously uncorrelated factor innovations that span the dominant subspace of variation in S_{it}. We work with standardized shocks series to prevent any single characteristic from dominating the common component.

The number of common factors is set to $r = 3$ based on a combination of empirical diagnostics: (i) the visual "elbow" in the scree plots, (ii) the eigenvalue ratio statistic of Ahn and Horenstein (2013), and (iii) the information criteria of Alessi et al. (2010). As shown in Figure 4, the first factor explains a sizable but incomplete share of total variance, typically below 60%. For example, in Germany the first component accounts for roughly 40%, while in most other units it captures about 50%, with Chile as the only case exceeding 65%. Across units, the diagnostics consistently indicate $r \in \{3, 4\}$. For parsimony and cross-country comparability, we fix $r = 3$, which is the smallest value ensuring at least 80% cumulative explained variance in all cases. The resulting factors are plotted in Figure 5.

Interpretation. Figure 6 reports the factor loadings obtained by regressing each individual temperature–shock on the three extracted factors. The overall fit of these regressions is satisfactory, with R^2 values exceeding 0.75 in all cases. Since factors are identified up to sign, we normalize their orientation to yield a consistent economic–climatic interpretation. The loading structure display a remarkable similarity across units. The first factor loads with the same sign on the mean and on all quantiles (normalized here to be positive). We interpret it as a *distributional shift* or *location* factor—an innovation that shifts the entire temperature distribution in the same direction as its mean. Physically, such shifts are consistent with global radiative imbalances at the top of the atmosphere caused by changes in greenhouse gas concentrations, volcanic aerosols, or solar activity (Hansen et al., 2005; Trenberth et al., 2014). The heterogeneous loading magnitudes across quantiles indicate that warming is not distributionally uniform globally and at the country-levels, consistent with the evidence in Gadea and Gonzalo (2020, 2025).

The second factor displays opposite signs for the mid-lower and mid-upper quantiles, with little or no loading on the mean. We interpret it as a *variability* factor, normalized so that cold quantiles become colder while warm quantiles become warmer. This pattern reflects internal modes of climate variability—such as the El Niño–Southern Oscillation (ENSO), the North Atlantic Oscillation (NAO), or the Pacific Decadal Oscillation (PDO)—which redistribute thermal energy across the planet and alter the variance of local temperatures without systematically affecting the global mean

[6] See **?** an for foundations of static PC factor extraction in large-N systems and **?** for a survey.

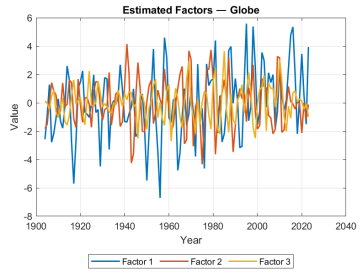


(a) Globe (b) United States (c) Germany

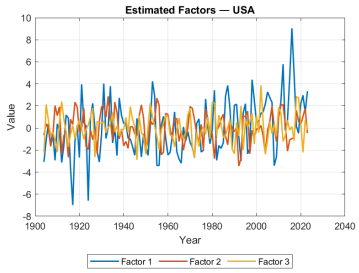
(d) France (e) Spain (f) Switzerland

(g) Norway (h) Mexico (i) Chile

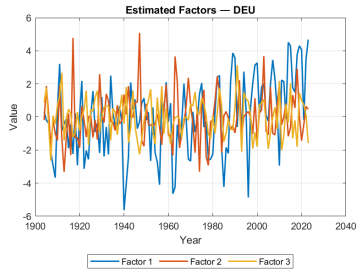
Figure 4: Screeplots of shock matrices



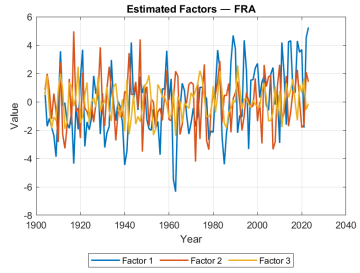
(a) Globe



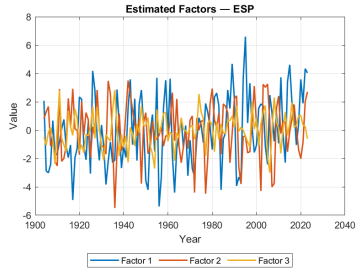
(b) United States



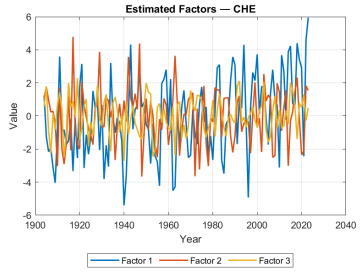
(c) Germany



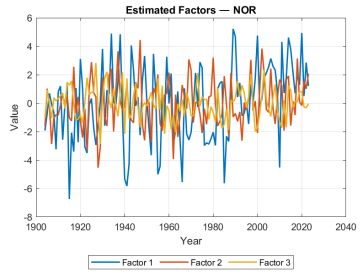
(d) France



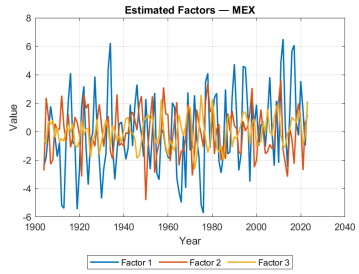
(e) Spain



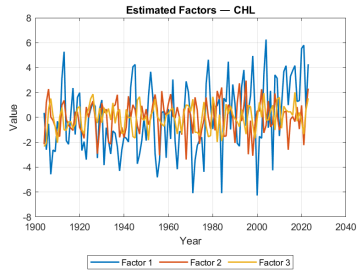
(f) Switzerland



(g) Norway



(h) Mexico



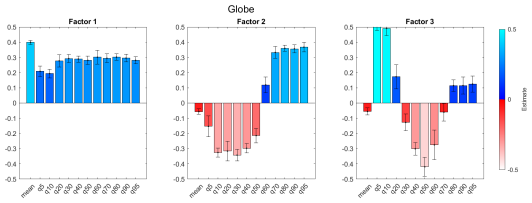
(i) Chile

Figure 5: Estimated factors

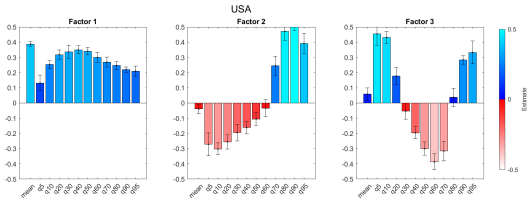
(Knutti and Rugenstein, 2015). The third factor loads positively on both tails and negatively at central quantiles, indicating a reallocation of probability mass from the center of the temperature distribution toward its tails. We interpret this as an *extremes* factor. Under our normalization, low quantiles rise (fewer cold events) while upper quantiles also increase (more hot events), implying that temperatures spend less time near typical values and more time in extreme states. This pattern reflects the documented widening of the global temperature distribution despite the asymmetric warming of cold and hot extremes (e.g., Hansen et al., 2005; Donat et al., 2013; Seneviratne et al., 2021).

Interpretations are further supported by the evidence reported in Table 3, which summarizes the estimated coefficients from regressions of several temperature distributional characteristics on the identified factors. Across all countries, the first factor (*distributional shift*) is positively associated with changes in the mean and with increases in both the maximum and minimum temperatures, but negatively related to dispersion measures such as the standard deviation (std) and the interquartile (iqr) range. This pattern implies that warming is not uniform across the temperature distribution: lower quantiles (minimums) tend to rise more rapidly than upper ones (maximums), consistent with the recent "warming amplification" evidence in Gadea and Gonzalo (2025). The second factor (*variability*) displays no systematic relationship with the mean but produces a consistent decline in dispersion measures across units, reinforcing its interpretation as capturing variations in the spread or variability of temperature distributions. Finally, the third factor (*extremes*) is typically associated with simultaneous increases in both minimums and maximums. It tends to raise skewness.

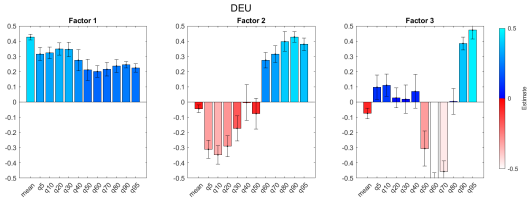
Two remarks follow. First, the three-factor structure and its qualitative interpretation emerge directly from the data without imposing sign or exclusion restrictions beyond standard factor-model normalizations, reinforcing that mean, variability, and extremes constitute distinct common drivers of temperature distributional shocks. Second, the need for more than one factor is consistent with recent evidence that a single average-temperature driver is insufficient to summarize temperature dynamics and their macroeconomic relevance (e.g., distribution- or season-specific shocks in Cipollini et al., 2023). These findings are also aligned with Boss and Testa (2025), who show for the United States that a single average-factor does not adequately represent temperature dynamics. Our results generalize this conclusion to the global level and to other countries.



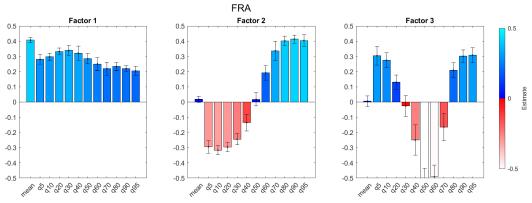
(a) Globe



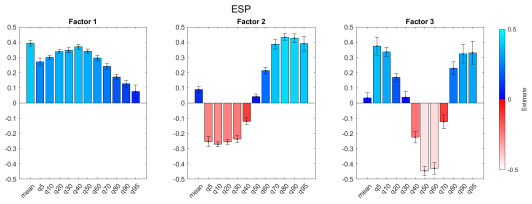
(b) United States



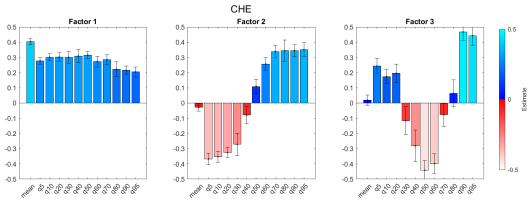
(c) Germany



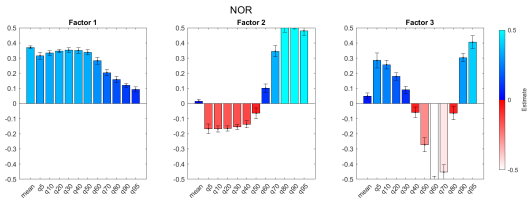
(d) France



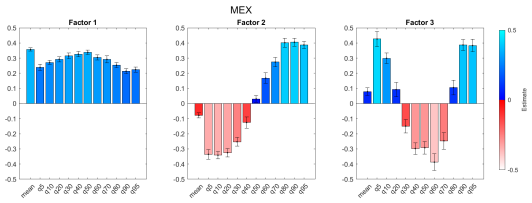
(e) Spain



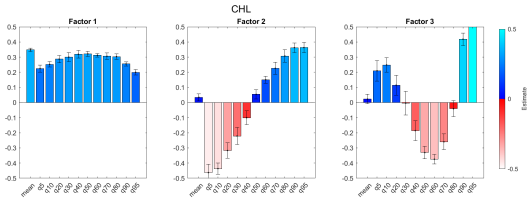
(f) Switzerland



(g) Norway



(h) Mexico



(i) Chile

Figure 6: Factor loadings

Table 3: Regression of temperature characteristics on identified factors

Global (World)				United States (USA)				Germany (DEU)			
	F1	F2	F3		F1	F2	F3		F1	F2	F3
mean	0.050***	-0.002	-0.009	mean	0.102***	0.011	0.026	mean	0.203***	0.023	-0.111*
max	0.081***	0.035*	0.040	max	0.166***	-0.171**	0.044	max	0.305***	-0.417***	0.423***
min	0.091***	0.083***	0.173***	min	0.390***	0.572***	0.841***	min	0.668***	0.656***	0.201
std	-0.032***	0.056***	-0.051***	std	-0.064***	-0.189***	-0.154***	std	-0.127***	-0.345***	-0.052
iqr	-0.094***	0.129***	-0.031	iqr	-0.115***	-0.296***	-0.100**	iqr	-0.222***	-0.579***	-0.283***
kur	0.009***	-0.016***	-0.005	kur	0.011	0.012	-0.039***	kur	-0.007	-0.004	0.043***
skw	-0.004***	0.007***	0.009***	skw	-0.001	-0.001	0.046***	skw	0.030***	0.017	0.086***
ctw	0.003***	-0.004***	-0.007***	ctw	0.003**	-0.001	-0.001	ctw	-0.002	-0.005*	0.001
France (FRA)				**Spain (ESP)**				**Switzerland (CHE)**			
	F1	F2	F3		F1	F2	F3		F1	F2	F3
mean	0.164***	-0.006	-0.100**	mean	0.116***	-0.017	0.009	mean	0.188***	0.026	-0.120**
max	0.259***	-0.338***	0.259***	max	0.099***	-0.181***	0.278***	max	0.291***	-0.365***	0.462***
min	0.434***	0.452***	0.518***	min	0.241***	0.237***	0.449***	min	0.433***	0.575***	0.382***
std	-0.042**	-0.248***	-0.053	std	-0.022**	-0.121***	0.010	std	-0.046**	-0.285***	0.008
iqr	-0.089**	-0.451***	-0.048	iqr	-0.035	-0.269***	0.037	iqr	-0.090**	-0.578***	-0.139
kur	-0.000	0.033***	-0.018*	kur	-0.003	0.021***	0.001	kur	0.000	0.014**	0.009
skw	0.015***	0.001	0.104***	skw	-0.007**	0.007	0.057***	skw	0.011**	0.022***	0.093***
ctw	-0.001	0.000	0.000	ctw	-0.003	-0.004*	-0.006	ctw	0.001***	0.001**	0.000
Norway (NOR)				**Mexico (MEX)**				**Chile (CHL)**			
	F1	F2	F3		F1	F2	F3		F1	F2	F3
mean	0.233***	-0.034	-0.032	mean	0.057***	0.013	0.037	mean	0.069***	-0.005	0.001
max	0.118***	-0.392***	0.408***	max	0.147***	-0.047	0.147*	max	0.028*	-0.044	0.123***
min	0.688***	0.374***	0.679***	min	0.171***	0.200***	0.476***	min	0.150***	0.162**	-0.064
std	-0.177***	-0.258***	-0.144**	std	-0.025***	-0.084***	-0.055***	std	-0.004	-0.098***	0.013
iqr	-0.326***	-0.520***	-0.431***	iqr	-0.038***	-0.150***	-0.037	iqr	0.021**	-0.162***	-0.075***
kur	0.018***	0.034***	0.020	kur	0.003	0.012**	-0.043***	kur	-0.011***	0.030***	0.037***
skw	0.005	-0.016**	0.097***	skw	0.003*	-0.001	0.041***	skw	-0.001	0.013**	0.054***
ctw	-0.003***	-0.001	-0.001	ctw	0.003***	0.005***	0.002	ctw	-0.003***	0.005**	-0.004**

Notes: Each panel reports the coefficients of an OLS regression of the form $y_t = \alpha + \beta F_{jt}$, where y_t is the corresponding characteristic and F_{jt} is the factor, $j = 1, 2, 3$. Newey-West standard errors used for inference. Significance: * $p < 0.10$, ** $p < 0.05$, *** $p < 0.01$.

4.2 Macroeconomic Effects of Temperature Distributional Shocks

4.2.1 Local Temperature Distributional Shocks

Figures A1, A2, and A3 in the Appendix report cumulative impulse responses of (log) GDP per capita, (log) TFP, and (log) CPI respectively, to selected individual Hamilton-filtered shocks extracted from local temperature distributions.[7] Responses to shocks to the average are qualitatively consistent with the related empirical literature (e.g., Dell et al., 2012; Hsiang, 2016; Nath et al.,

[7]Each individual shock series is standardized to facilitate comparison across characteristics. For completeness, the temperature-characteristic IRFs to their own shocks are reported in the Online Appendix.

2024): a one–standard deviation innovation to the country-level mean temperature generally induces a persistent and statistically significant decline in cumulative GDP per capita and TFP growth. Shocks to other distributional characteristics also yield statistically significant effects, with patterns that are country-specific.

Several cases are worth highlighting. In the United States, for example, GDP responses to both the average and the selected quantile shocks are negative and statistically significant through the full horizon ($h = 10$). A qualitatively similar pattern is obtained for Germany and Switzerland. In Spain, in contrast, GDP responses do not rule out a zero effect at all horizons, suggesting a preliminary limited short- to medium-term macroeconomic sensitivity to the analyzed temperature innovations. A similar conclusion holds for Chile. In Norway, we observe a negative and significant response only for shocks to the 0.90 quantile, whereas in France significance concentrates at the 0.10 quantile. Country-specific figures for all characteristics and dependent variables are reported in the Online Appendix, where readers can inspect any country of interest.

Given the correlation structure among individual shocks documented in Section 4.1, it is not possible to infer from the one-by-one analysis which characteristics are driving the observed macroeconomic responses, or whether an average-temperature shock is sufficient to summarize broader distributional effects. We therefore turn to the three identified orthogonal local factor shocks, capturing *average*, *variability*, and *extremes* shifts in country-level temperature distributions. To aid interpretation and benchmark response magnitudes, Figure 7 reports the impulse responses of local temperature characteristics to a one-unit innovation in each estimated factor. The shapes of these responses align with the loading-based interpretation: Factor 1 induces a broad location shift, Factor 2 raises dispersion via opposite tail movements, and Factor 3 reallocates probability mass from the center toward the tails. Because our LP specifications are linear in the shock, local-factor responses can be linearly rescaled to any target temperature change.[8] For example, if a one-unit shock to local factor m raises the local average (or a given quantile) by $\Delta_i^{(m)}$ degrees in country i, then the corresponding IRFs for a 1°C change in that characteristic are obtained by multiplying the reported IRFs by $1/\Delta_i^{(m)}$:

$$\mathrm{IRF}_{i,l}\big(1^{\circ}\mathrm{C}\big) \;=\; \frac{1}{\Delta_i^{(m)}}\,\mathrm{IRF}_{i,l}\big(\text{one-unit factor } m\big).$$

For illustration, in the United States, a one-unit innovation to Factor 1 raises the local average temperature by approximately 0.18°C on impact: normalizing to a 1°C increase therefore entails

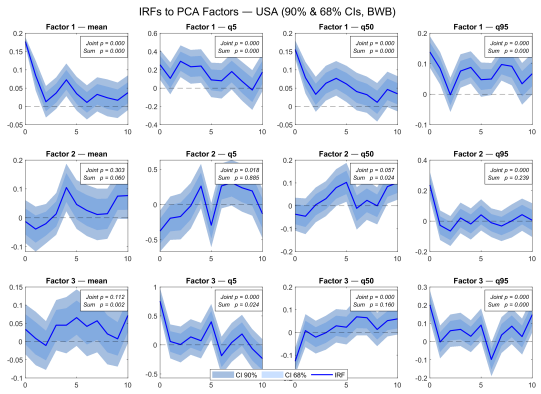
[8] Rescaling is valid under the maintained linearity of local projections with respect to the shock. If one adopts state-dependent LPs or allows for non-linear effects, the mapping between shock size and response may itself be state- or level-dependent.

dividing the reported IRFs by 0.18.

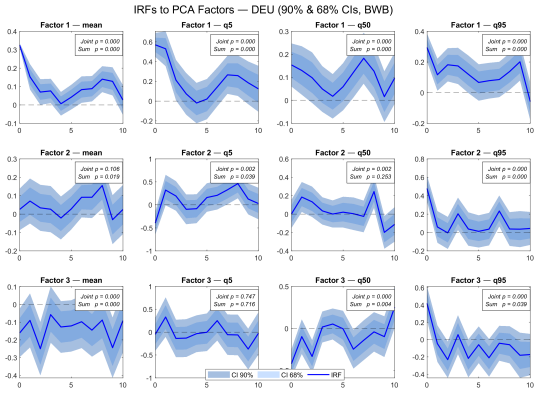
Output. The dependent variable is (log) real GDP per capita. We estimate impulse responses using the cumulative-type local projection in Equation (4), so that coefficients trace the effect of a one–unit increase in the relevant factor shock on the cumulative growth rate of GDP per capita h periods ahead, for $h = 0, 1, \ldots, 10$. The right-hand side of the LP regression includes: (i) the factor shock at t, (ii) two lags of that factor shock, and (iii) two lags of real GDP per capita growth. To account for global business-cycle fluctuations, we also include two lags of global oil price inflation and a set of World Bank global recession dummies. Figure 8 reports country-specific responses. Solid lines are point estimates; shaded bands denote 90% (dark) and 68% (light) confidence intervals computed via a heteroskedasticity- and autocorrelation-robust wild bootstrap. For each panel, we additionally report a Wald p-value for the joint significance of the local projection coefficients across horizons, and a p-value for the restriction that the cumulative effect (sum across horizons) equals zero.

A one–unit shock in the *distributional shift* local factor (Factor 1) induces a significant and persistent decline in the cumulative growth rate of GDP per capita in the United States, Germany, France, Switzerland, and Mexico. For the United States, the response reaches a peak of approximately -0.94 percentage points at horizon $h = 10$. Scaling by the corresponding change in the local mean temperature of 0.18°C, the implied effect of a 1°C increase in average temperature is roughly -5.2%. The magnitudes for other countries can be interpreted analogously, keeping in mind that the local temperature responses—and thus the scaling factors—differ across locations. In Spain, Norway, and Chile, output responses to Factor 1 are not jointly significant, although in Spain the IRF remains negative across all horizons and the cumulative sum is marginally significant. Overall, the evidence for the distributional shift factor is consistent with the established literature documenting contractionary output effects of mean-temperature shocks. Our main contribution is to extend this analysis to the *variability* (Factor 2) and *extremes* (Factor 3) factors, which capture changes in higher moments of the temperature distribution.

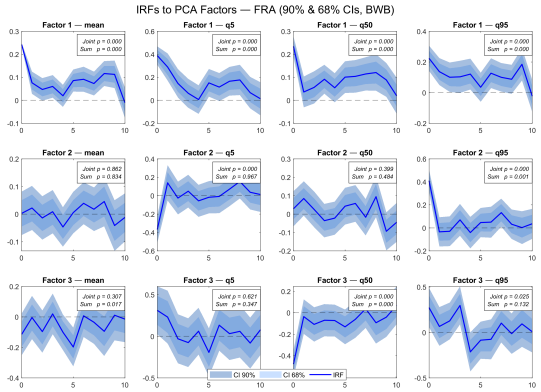
For the United States, the *distributional shift* factor alone is sufficient to explain the output responses to changes in the local temperature distribution: impulse responses of cumulative GDP growth to *variability* (Factor 2) and *extremes* (Factor 3) factors are not statistically significant at any horizon. This pattern contrasts with those observed in other economies. In France and Switzerland, for example, shocks to both *variability* and *extremes* generate persistent and significant cumulative GDP growth declines. In Germany and Mexico, a unit-increase in the *variability* factor similarly depresses GDP growth, whereas in Norway the same type of shock produces a positive



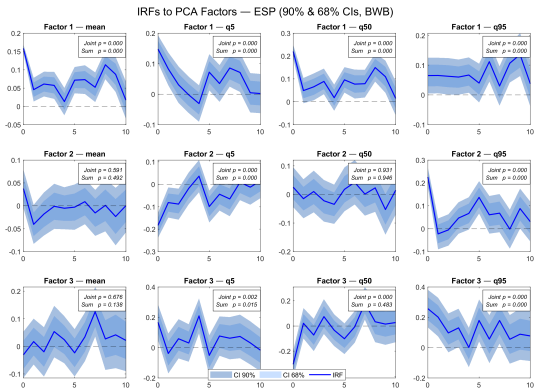
(a) United States



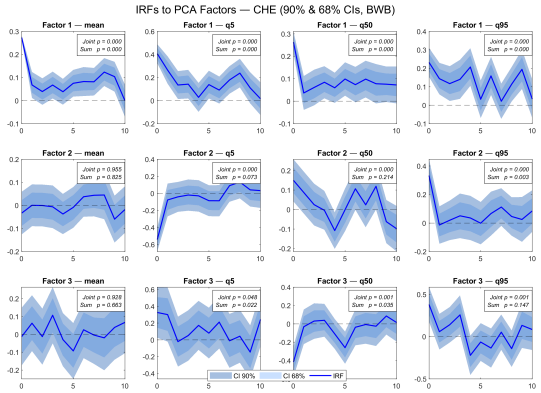
(b) Germany



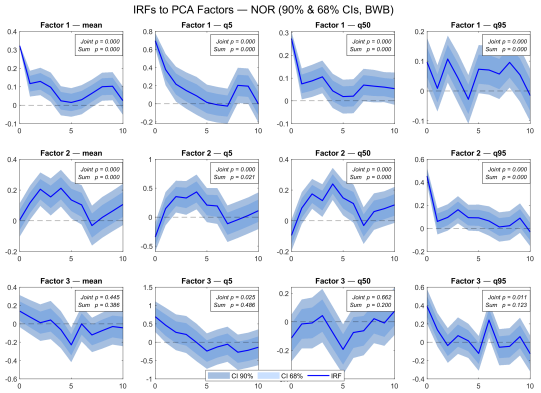
(c) France



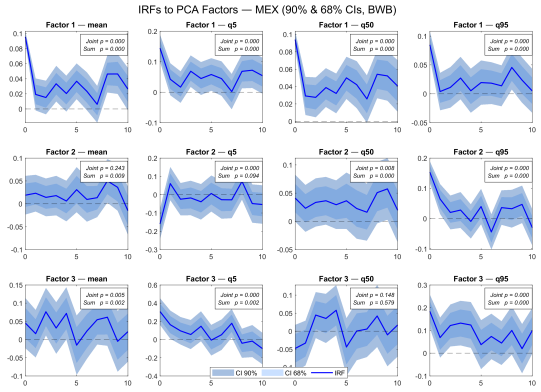
(d) Spain



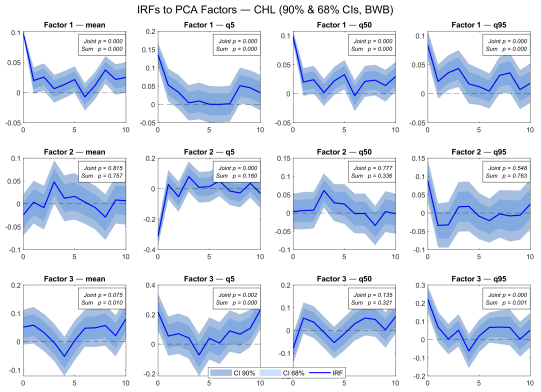
(e) Switzerland



(f) Norway



(g) Mexico



(h) Chile

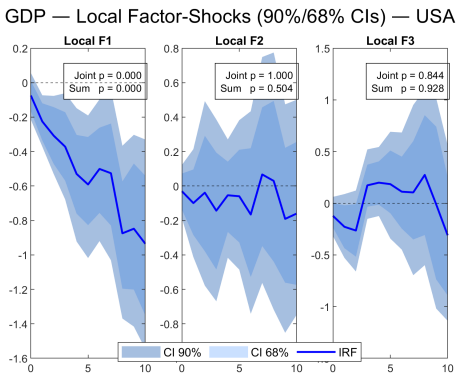
Figure 7: Local temperature responses to local factor shocks

and statistically significant response. A particularly illustrative case is Spain, where a shock that amplifies the *extreme tails* of the temperature distribution leads to a significant contraction in GDP growth. Specifically, a shock increases the local 0.05 quantile by 0.19°C and the 0.95 quantile by 0.22°C, induces an output decline of roughly $-\%$ at horizon $h = 10$. Such effects would be entirely missed in analyses restricted to mean-temperature or *distributional-shift* shocks, underscoring the value of modeling temperature heterogeneity across the entire distribution.

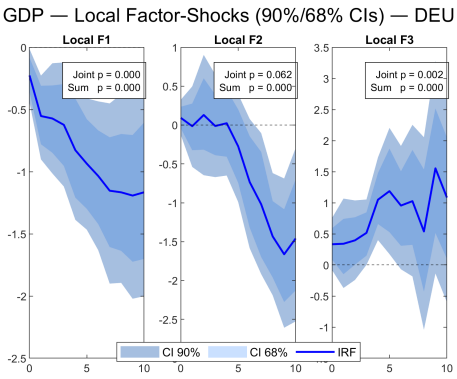
Total Factor Productivity. We next examine how local temperature distributional shocks affect total factor productivity, a key transmission mechanism for the macroeconomic risk of climate change. The dependent variable is (log) TFP, with the TFP measure taken from Bergeaud et al. (2016). Figure 9 reports cumulative-type impulse responses, which trace the effect of a one–unit increase in each local factor on the cumulative growth rate of TFP h years ahead. The response patterns closely mirror those described for GDP per capita. Specifically, the *distributional shift* factor (Factor 1) induces a significant and persistent decline in cumulative TFP growth in nearly all countries, except Norway and Chile. In Spain, for example, we now observe a pronounced and statistically significant TFP contraction consistent with the negative GDP responses, although the latter were only weakly significant under the sum test. The contractionary TFP effects of the *distributional shift* factor are consistent with the standard empirical literature based on mean-temperature shocks.

Turning to the other two factors, responses remain heterogeneous across countries. A significant decline in TFP growth following an increase in temperature *variability* (Factor 2) is observed for Germany, France, Switzerland, and Mexico. For the United States, although not jointly significant, the IRF is positive and upward trending beyond horizon $h > 3$, and the sum-of-coefficients test rejects the null of zero cumulative effects. A similar, and more pronounced, positive response to increased *variability* is found for Norway. Regarding the *extremes* factor (Factor 3), responses are negative and jointly significant for the same set of countries as in the GDP case: France, Spain, and Switzerland. In contrast, for Germany and Mexico, a shock amplifying the temperature tails produces a positive effect on TFP, consistent with the GDP expansion observed in the former case. For Chile, changes in the local temperature distribution appear to have no significant effect on TFP growth.

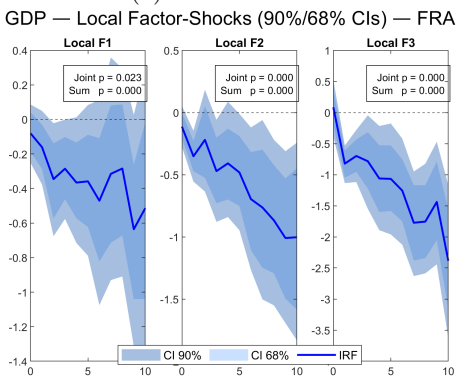
Prices. Figure 10 presents the cumulative impulse responses of inflation to the identified local factor shocks. The dependent variable in this case is the (log) CPI. Shocks to the *distributional shift* factor generate a decline in prices in nearly all economies. Comparing these results with the corresponding GDP responses, this pattern suggests that the *distributional shift* shock operates



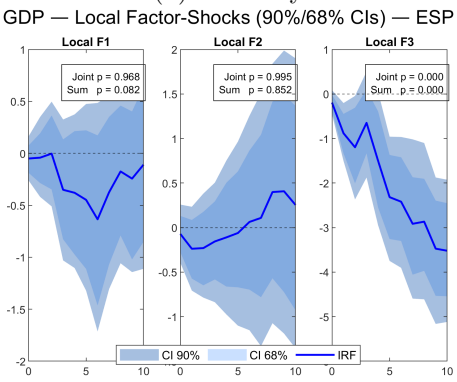
(a) United States



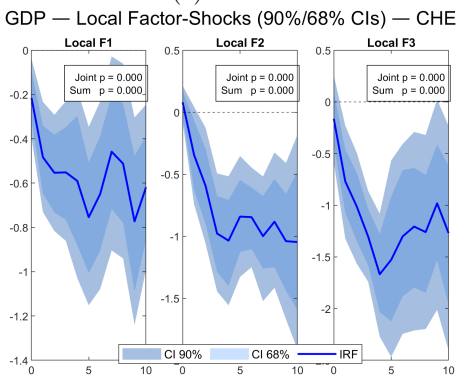
(b) Germany



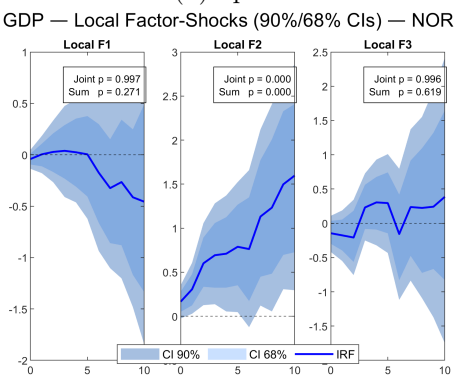
(c) France



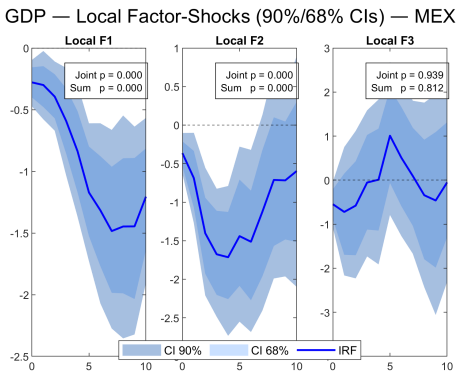
(d) Spain



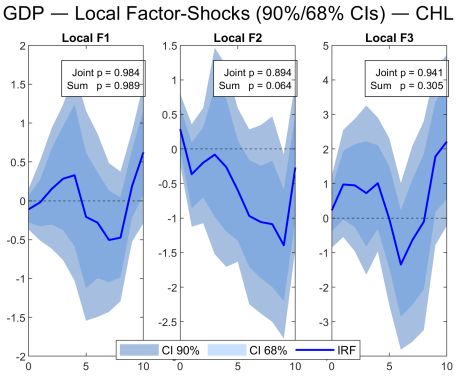
(e) Switzerland



(f) Norway

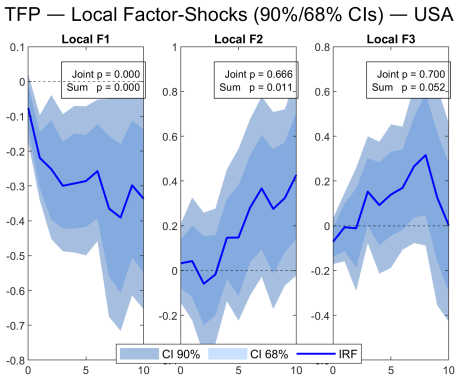


(g) Mexico

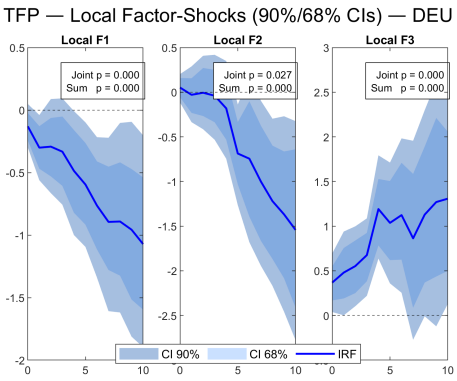


(h) Chile

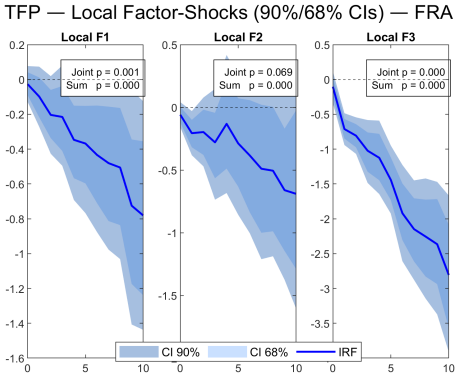
Figure 8: GDP per-capita growth responses to local factor shocks



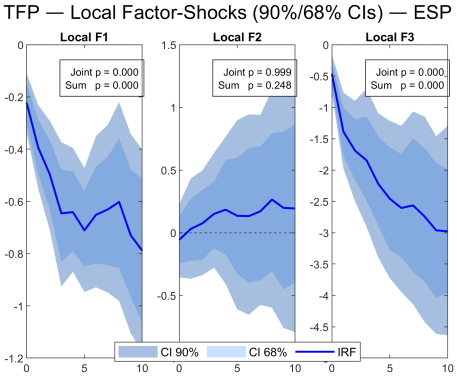
(a) United States



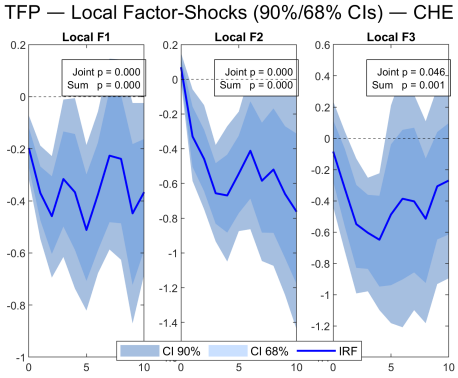
(b) Germany



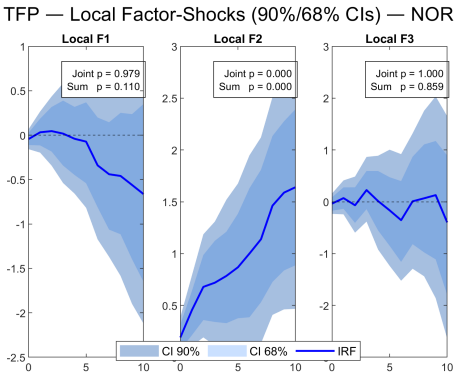
(c) France



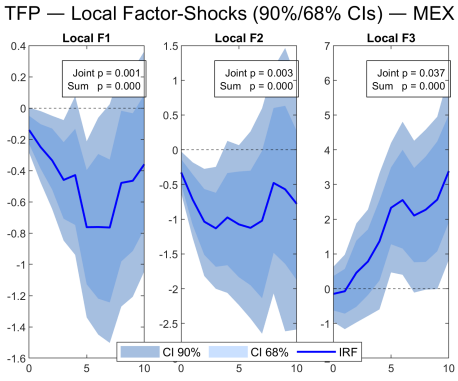
(d) Spain



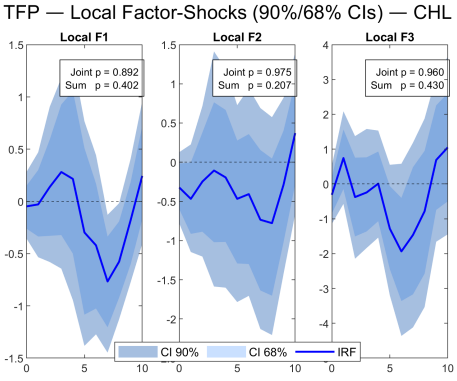
(e) Switzerland



(f) Norway



(g) Mexico



(h) Chile

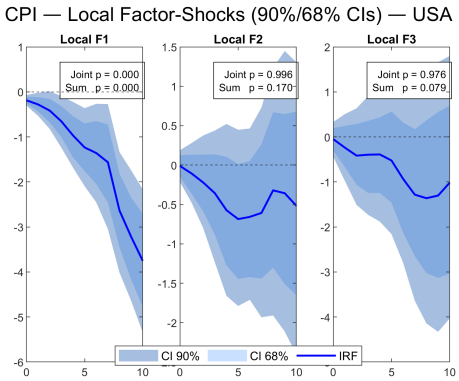
Figure 9: TFP growth responses to local factor shocks

primarily as a demand-type disturbance in countries such as the United States, Germany, France, Spain, and Switzerland, where output growth also falls. This finding aligns with the hypothesis that physical climate risks tend to propagate as demand-type shocks by depressing aggregate spending and investment, as argued by Ciccarelli and Marotta (2024). The *extremes* factor similarly behaves as a demand-type shock in Germany, where inflation increases in tandem with GDP growth and the responses are jointly significant. By contrast, the *variability* factor exhibits weak evidence of supply-type behavior in Germany, France, and Switzerland—raising prices while reducing output—although price effects are only mildly significant.

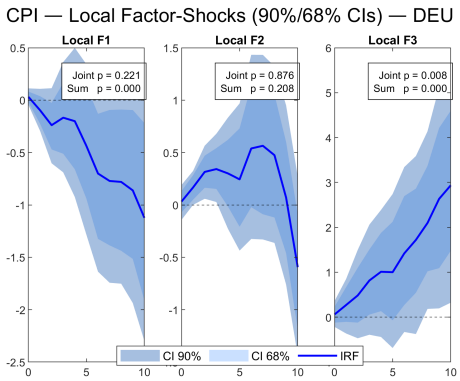
Some country-specific cases are noteworthy. In Mexico, a significant fall in prices is observed only for the *extremes* factor, which, interestingly, has no significant impact on GDP. In Chile, where output responses are not statistically significant, Factors 1 and 3 produce a strong decline in cumulative inflation, suggesting that temperature shocks may affect local price dynamics through channels unrelated to domestic activity—such as expectations or imported energy prices. Norway displays a similar pattern: while output responds only to the *variability* factor, inflation reacts significantly to Factors 1 and 3. Such divergences between output and price responses may arise whenever temperature shocks affect either production capacity or demand conditions: shocks that constrain supply but leave demand unchanged tend to raise prices with limited output effects, while shocks that depress demand through confidence or investment channels reduce output without necessarily generating inflationary pressure.

4.2.2 Global Temperature Distributional Shocks

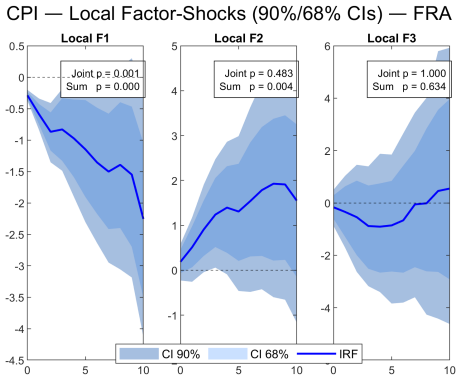
Bilal and Känzig (2024) and Neal (2023) emphasize the importance of accounting for global temperature changes when estimating the economic damages from climate change. The mechanisms through which global and local temperatures affect country-level economic activity, are distinct and so are their macroeconomic responses. A global average-temperature shock influences domestic economic outcomes through multiple channels. First, it changes the local temperature distribution directly. Second, as documented by Bilal and Känzig (2024), it correlates with large-scale climatic disruptions such as droughts, extreme winds, or heavy precipitation, that have disproportionate effects on output. Shifts in other parts of the global temperature distribution entail other types of physical and economic consequences that propagate through trade, capital reallocation, and cross-border production linkages. Against this background, this section examines the macroeconomic responses to global temperature distributional shocks that are common across all countries in the sample.



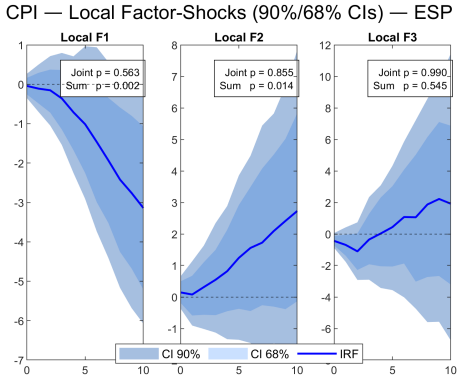
(a) United States



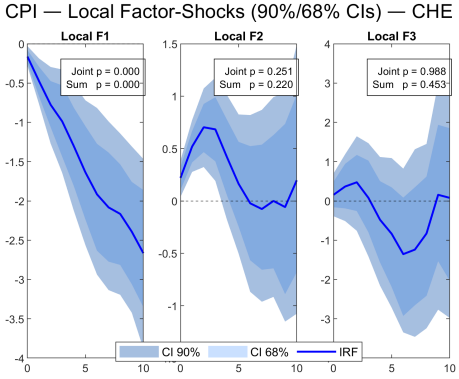
(b) Germany



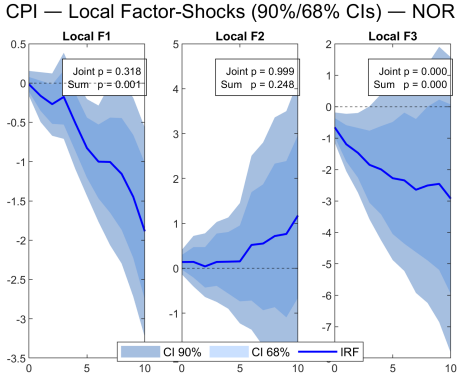
(c) France



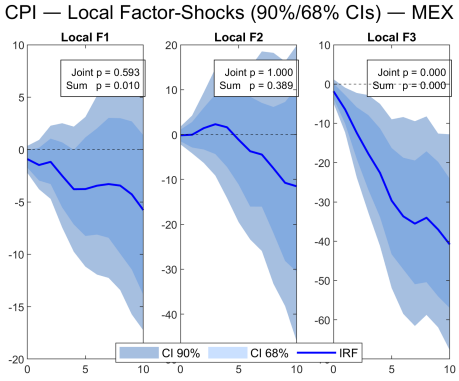
(d) Spain



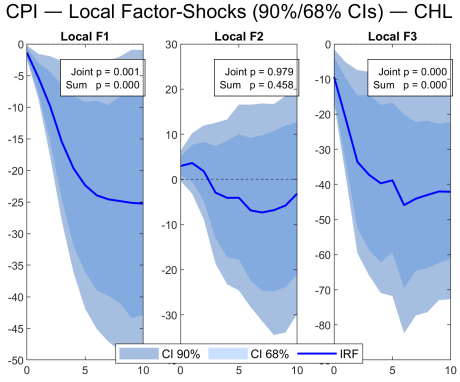
(e) Switzerland



(f) Norway



(g) Mexico



(h) Chile

Figure 10: Inflation responses to local factor shocks

Figures A4, A5, and A6 in the Appendix display the cumulative impulse responses of (log) GDP per capita, (log) TFP, and (log) CPI respectively, to selected individual Hamilton-filtered shocks obtained from the global temperature distribution. Similar to the local-shocks analysis, responses to average-temperature innovations are qualitatively consistent with Bilal and Känzig (2024) and related studies: a shock increasing the global mean temperature generates a statistically significant and persistent decline in cumulative GDP per capita and TFP growth across nearly all countries. Other distributional characteristics also produce statistically significant responses, although their direction and persistence vary by country. Given the strong contemporaneous correlation among individual temperature shocks, we next extract the three *orthogonal* global factor shocks summarizing the main sources of common variation across the temperature distribution and study their macroeconomic effects. Figure 11 reports the corresponding impulse responses of global temperature characteristics to each factor. The first global factor increases the global mean by approximately 0.089°C on impact, with stronger effects at lower quantiles. Similarly, Factor 3 is associated with relatively larger movements in the lower tail. These magnitudes provide the scale for interpreting the downstream macroeconomic responses. Because the LP specifications are linear in the shock, IRFs can be linearly rescaled to any desired shock size (e.g., a 1°C change in the mean or in a given quantile).

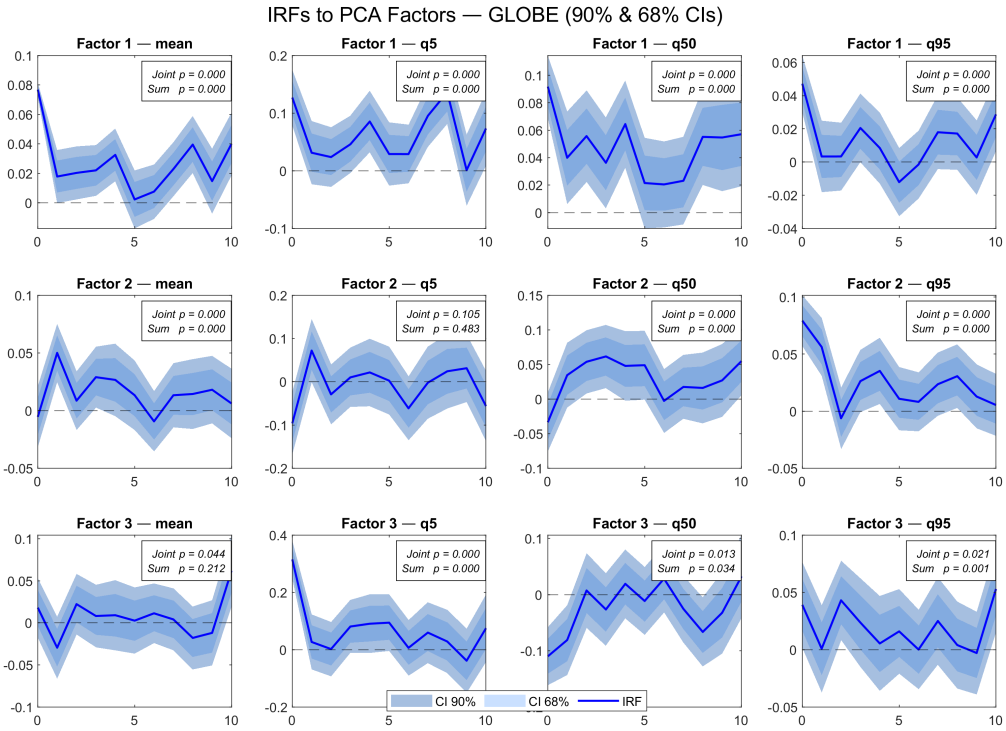


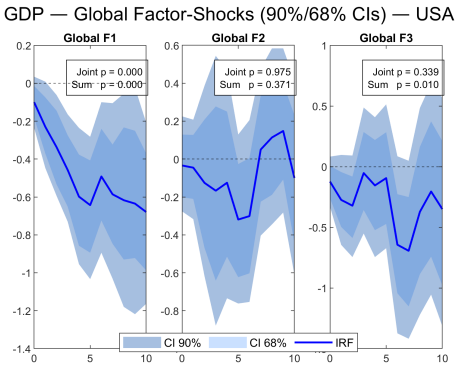
Figure 11: Global temperature responses to global factor shocks

Output. Figure 12 reports country-specific cumulative impulse responses of GDP per capita

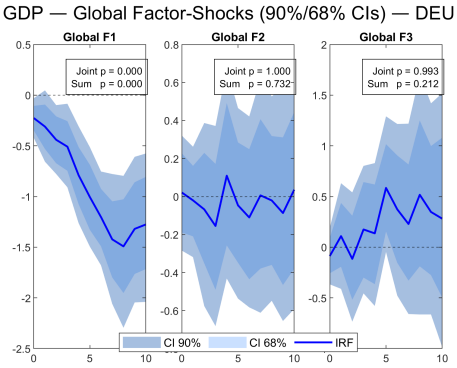
to each global factor shock. A one–unit shock in the *distributional shift* factor (Factor 1) induces a significant and persistent decline in the cumulative growth rate of GDP per capita across all countries in the sample, with the sole exception of Chile. For the United States, the response reaches approximately -0.64 percentage points at horizon $h = 5$. Scaling by the corresponding change in global mean temperature of 0.089°C, the implied effect of a 1°C increase in average temperature is roughly -7.2%, a magnitude closely aligned with the estimates of Bilal and Känzig (2024). Similar or even stronger contractionary effects are observed for Germany, Norway, Spain, and Mexico. The result for Spain contrasts with the null output effect of the local Factor 1 reported in the previous section, highlighting that global and local shocks operate through distinct transmission mechanisms. Overall, the evidence for the *distributional shift* factor corroborates the established literature documenting negative output impacts of global mean temperature shocks.

The responses to the *variability* (Factor 2) and *extremes* (Factor 3) factors—our key contribution to the literature—are markedly heterogeneous across countries. A one–unit innovation in the *variability* factor, characterized by an increase in the dispersion of global temperature distribution, generates a jointly significant and positive cumulative GDP response in Switzerland and Spain. In France, the IRF is positive at all horizons, while in Norway it is negative: in both cases, the effects are not jointly significant, though the sum test rejects the null of zero cumulative impact. The *extremes* factor, associated with a relative increase in temperature extremes—particularly at the colder end of the distribution—also displays heterogeneous responses. For France and Switzerland, a one–unit increase in this factor yields a statistically significant and positive impact on cumulative GDP growth, whereas in Norway the response is negative. For Chile, none of the three global factors produce jointly significant IRFs.

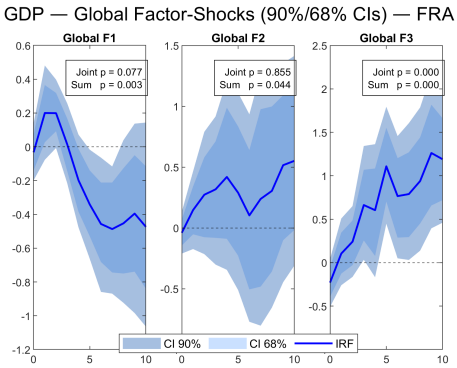
Total Factor Productivity. Figure 13 reports the cumulative impulse responses of TFP growth to the identified global factor shocks. The results largely mirror those for GDP per capita growth, suggesting that productivity acts as a key transmission mechanism linking temperature shocks to aggregate output. A one-unit increase in the *distributional shift* factor (Factor 1) induces a significant and persistent decline in TFP growth across all countries except Chile. IRFs are jointly significant and of magnitudes comparable to those observed for output in Figure 12. Shocks to the *variability* factor (Factor 2) generate heterogeneous effects: negative and statistically significant under the sum test in the United States, Germany, Norway, and Chile, negative and jointly significant in Norway, but positive and jointly significant in France and Spain. The *extremes* factor (Factor 3) produces further asymmetries, with positive cumulative effects in France, Switzerland, and Mexico, and a strong, persistent TFP contraction in Norway. In Chile, Factors 3 yields negative responses at horizons $h \geq 23$, though significance is achieved only under the sum test.



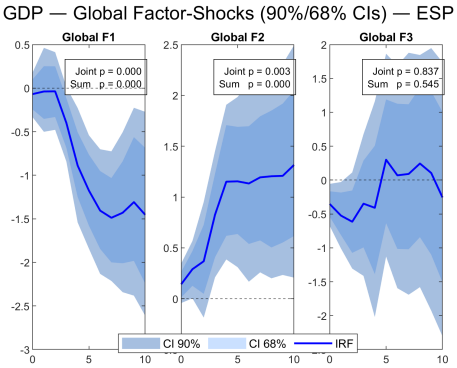
(a) United States



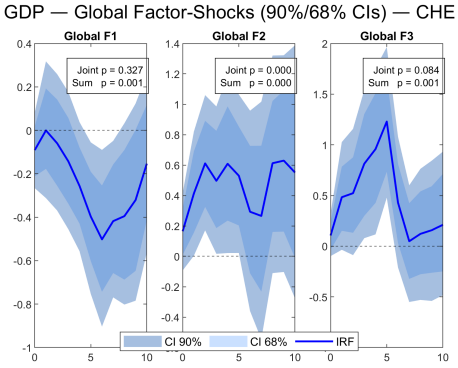
(b) Germany



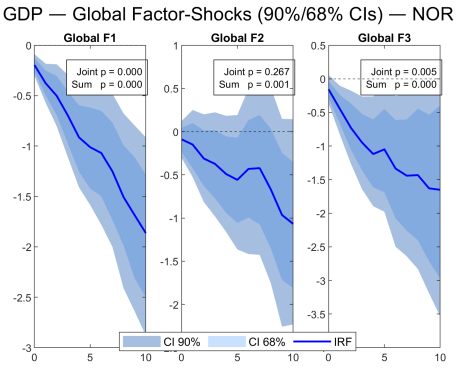
(c) France



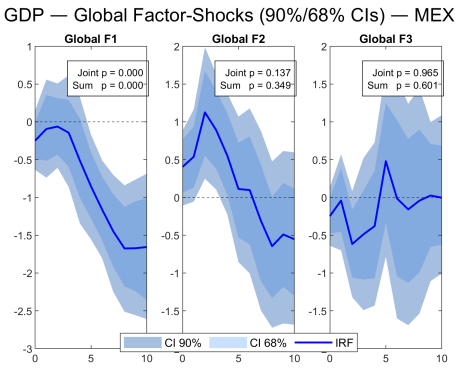
(d) Spain



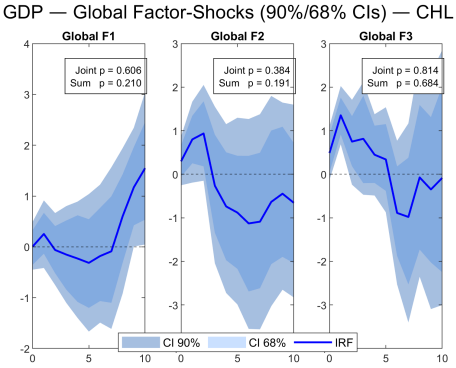
(e) Switzerland



(f) Norway

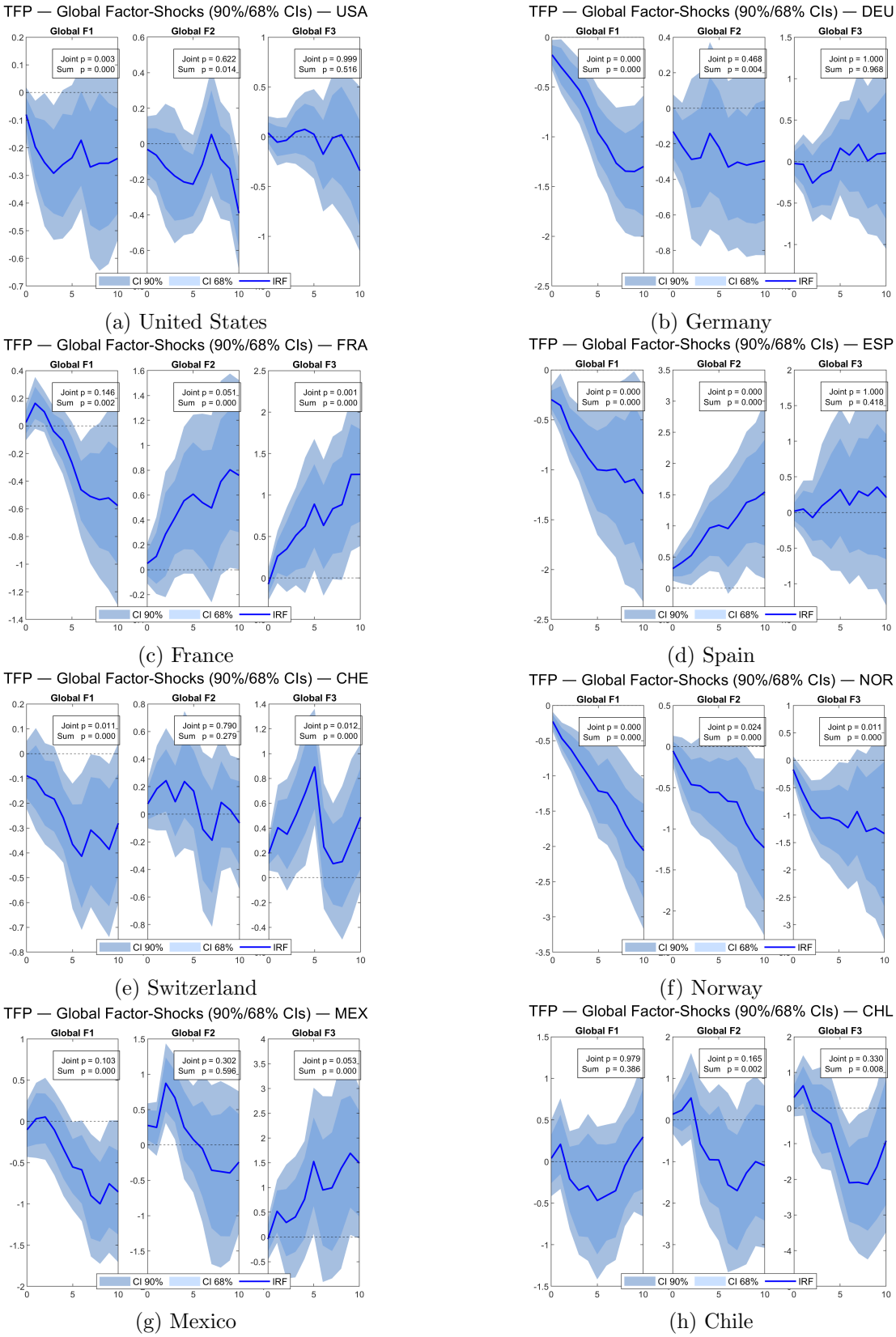


(g) Mexico



(h) Chile

Figure 12: GDP per-capita growth responses to global factor shocks



(a) United States (b) Germany

(c) France (d) Spain

(e) Switzerland (f) Norway

(g) Mexico (h) Chile

Figure 13: TFP growth responses to global factor shocks

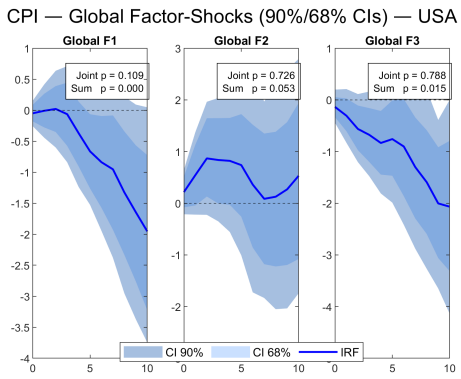
Prices. According to the evidence in Figure 14, global factor shocks predominantly behave as demand-side disturbances, as reflected in the same-sign responses of cumulative inflation and output growth. Specifically, the *distributional shift* factor induces price declines in the countries where it also reduces output, consistent with a contractionary demand impulse. The only exceptions are France, where the CPI response is positive and significant under the sum test, and Mexico, where the effect on prices is statistically insignificant. Similar readings can be made for the other global factors. For instance, in Spain, France, and Mexico, where the *variability* factor generates positive GDP responses, cumulative inflation also rises significantly (only under the sum test for Mexico). The *extremes* factor produces the same-sign movements pattern in output and prices. In a few cases, output responses are not accompanied by inflation changes—for example, Factor 2 in Switzerland and Factor 3 in France and Switzerland—suggesting weaker price transmission channels. In Chile, both Factors 1 and 3 significantly reduce prices despite the absence of significant output responses. Overall, the evidence supports the view that global temperature shocks operate primarily through demand-side channels, consistent with Ciccarelli and Marotta (2024). Nevertheless, caution is warranted, as analyses at higher frequency (e.g., monthly) or using alternative inflation measures, such as core or energy prices, may reveal different short-run dynamics.

4.3 Robustness and Additional Analyses

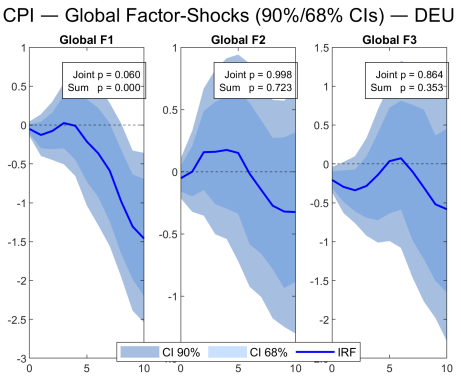
This section is currently being developed and will include a series of robustness exercises examining alternative definitions of temperature shocks and different identification schemes. Specifically, we will compute shocks as: (i) temperature deviations from the 30-year historical mean; (ii) residuals from a VAR of temperature characteristics; (iii) innovations from a multivariate version of the Hamilton filter. Our main results regarding the identified factor structure and macroeconomic responses remain robust across these choices. Additionally, we will study time variation in the estimated effects (see Kim et al. (2025) for a recent reference) by conducting a subsample analysis for the period 1901–1960 and estimating state-dependent local projections for 1960-2022 defining the indicator $I(t > 1990)$.

5 Conclusion

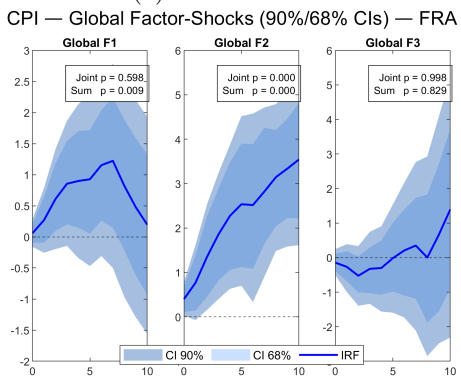
In this paper, we show that shocks affecting different parts of the temperature distribution matter for macroeconomic performance, and that focusing solely on average temperature overlooks critical sources of climate risk. Using gridded temperature data and macroeconomic indicators for the globe



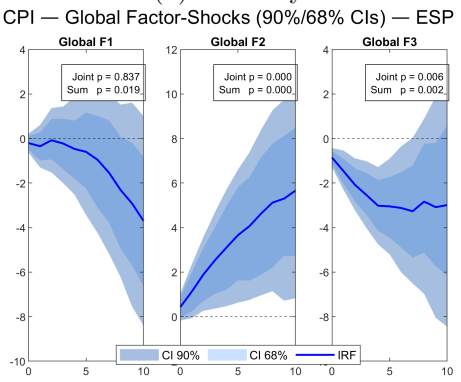
(a) United States



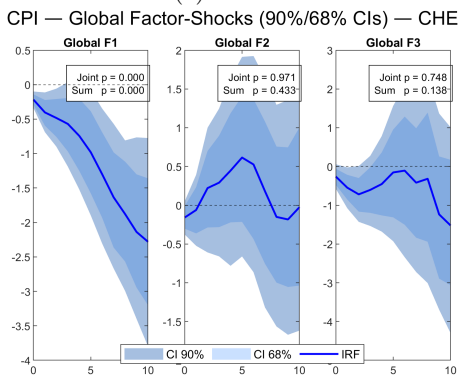
(b) Germany



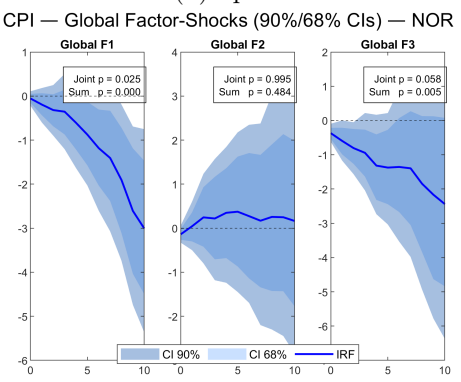
(c) France



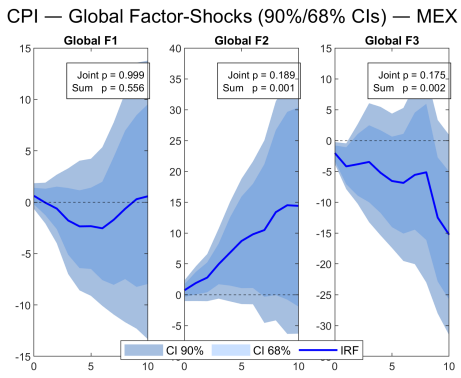
(d) Spain



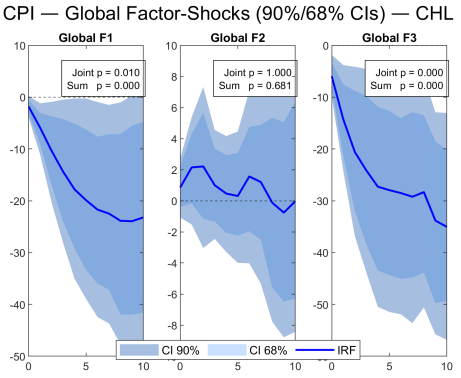
(e) Switzerland



(f) Norway



(g) Mexico



(h) Chile

Figure 14: Inflation responses to global factor shocks

and a set of 21 countries, we construct time series of temperature distributional characteristics and identify temperature distributional shocks following the most recent econometric procedures in the literature. A factor analysis applied to the full set of individual (local and global) distributional shocks consistently revealed three orthogonal factors that summarize the common sources of variation, all of them with significant macroeconomic implications. The first factor—interpreted as a *distributional shift* or *location* factor is associated with persistent declines in GDP per capita and total factor productivity, consistent with the literature treating average temperature as a sufficient statistic for climate risk. The second and third factors, which leave the mean unchanged but capture shifts in *variability* and *extremes*, produce additional and heterogeneous macroeconomic effects not document by the standard literature.

From a policy perspective, our findings highlight two main implications. First, estimates of the social cost of carbon based solely on mean temperature changes are likely to understate the true economic damages from climate change. Accounting for distributional shocks provides a more comprehensive measure of climate risk in a heterogeneous warming environment. Second, the cross-country heterogeneity in responses underscores the need for adaptation strategies that address not only gradual warming but also shifts in the frequency, persistence, and intensity of temperature extremes. Integrating the full temperature distribution into climate-macroeconomic models improves the assessment of economic vulnerability and enhances the design of effective mitigation and adaptation policies.

References

Ahn, S. C. and A. R. Horenstein (2013). Eigenvalue Ratio Test for the Number of Factors. *Econometrica 81*(3), 1203–1227.

Akyapı, B., M. Bellon, and E. Massetti (2025). Estimating Macrofiscal Effects of Climate Shocks from Billions of Geospatial Weather Observations. *American Economic Journal: Macroeconomics 17*(3), 114–159.

Alessandri, P. and H. Mumtaz (2025). The Macroeconomic Cost of Temperature Risk. *Journal of International Economics 158*, 104157.

Alessi, L., M. Barigozzi, and M. Capasso (2010). Improved Penalization for Determining the Number of Factors in Approximate Factor Models. *Statistics & Probability Letters 80*(23-24), 1806–1813.

AR6-IPCC (2021). *Climate Change 2021: The Physical Science Basis*. [Masson-Delmotte V, Zhai P, Pirani A et al. (eds)]. Cambridge and New York: Cambridge University Press.

Bai, J. and S. Ng (2002). Determining the Number of Factors in Approximate Factor Models. *Econometrica 70*(1), 191–221.

Bai, J. and S. Ng (2013). Principal Components Estimation and Identification of Static Factors. *Journal of econometrics 176*(1), 18–29.

Barrage, L. (2024). Climate Change Impacts on Public Finances Around the World. CESifo Working Paper Series 11443, CESifo.

Bergeaud, A., G. Cette, and R. Lecat (2016). Productivity Trends in Advanced Countries Between 1890 and 2012. *Review of Income and Wealth 62*(3), 420–444.

Bilal, A. and D. R. Känzig (2024, May). The Macroeconomic Impact of Climate Change: Global vs. Local Temperature. NBER Working Paper 32450, National Bureau of Economic Research, Inc.

Bilal, A. and J. H. Stock (2025, March). Macroeconomics and Climate Change. NBER Working Paper 33567, National Bureau of Economic Research, Inc.

Boss, K. and A. Testa (2025). What Goes Around Comes Around: The US Climate-Economic Cycle. *Journal of Macroeconomics*, 103680.

Brunner, L., G. C. Hegerl, and A. K. Steiner (2017). Connecting Atmospheric Blocking to European Temperature Extremes in Spring. *Journal of Climate 30*(2), 585–594.

Burke, M., W. M. Davis, and N. S. Diffenbaugh (2018). Large Potential Reduction in Economic Damages under UN Mitigation Targets. *Nature 557*(7706), 549–553.

Burke, M., S. M. Hsiang, and E. Miguel (2015). Global Non-linear Effect of Temperature on Economic Production. *Nature 527*(7577), 235–239.

Carleton, T., A. Jina, M. Delgado, M. Greenstone, T. Houser, S. Hsiang, A. Hultgren, R. E. Kopp, K. E. McCusker, I. Nath, et al. (2022). Valuing the Global Mortality Consequences of Climate Change Accounting for Adaptation Costs and Benefits. *The Quarterly Journal of Economics 137*(4), 2037–2105.

Chapman, S., D. Stainforth, and N. Watkins (2013). On Estimating Local Long-term Climate Trends. *Phil Trans R Soc A 371:20120287*.

Ciccarelli, M. and F. Marotta (2024). Demand or Supply? An Empirical Exploration of the Effects of Climate Change on the Macroeconomy. *Energy Economics 129*, 107163.

Cipollini, A., F. Parla, et al. (2023). Temperature and Growth: A Panel Mixed Frequency VAR Analysis Using NUTS2 Data. *Recent Workin Paper Series*.

Colacito, R., B. Hoffmann, and T. Phan (2019). Temperature and Growth: A Panel Analysis of the United States. *Journal of Money, Credit and Banking 51*(2-3), 313–368.

Dell, M., B. F. Jones, and B. A. Olken (2012, July). Temperature Shocks and Economic Growth: Evidence from the Last Half Century. *American Economic Journal: Macroeconomics 4*(3), 66–95.

Donadelli, M., M. Jüppner, and S. Vergalli (2022). Temperature Variability and the Macroeconomy: A World Tour. *Environmental and resource economics 83*(1), 221–259.

Donat, M., L. V. Alexander, H. Yang, I. Durre, R. Vose, R. J. Dunn, K. M. Willett, E. Aguilar, M. Brunet, J. Caesar, et al. (2013). Updated Analyses of Temperature and Precipitation Extreme Indices Since the Beginning of the Twentieth Century: The HadEX2 Dataset. *Journal of Geophysical Research: Atmospheres 118*(5), 2098–2118.

Faccia, D., M. Parker, and L. Stracca (2021, Dec). Feeling the Heat: Extreme Temperatures and Price Stability. Working Paper Series 2626, European Central Bank.

Feyen, L., J. C. Ciscar-Martinez, S. Gosling, D. Ibarreta-Ruiz, A. Soria-Ramirez, A. Dosio, G. Naumann, S. Russo, G. Formetta, G. Forzieri, et al. (2020). Climate Change Impacts and Adaptation in Europe: JRC PESETA IV Final Report. Scientific analysis or review, Damage assessment, Risk assessment KJ-NA-30180-EN-N (online), Luxembourg (Luxembourg).

Gadea, M. D. and J. Gonzalo (2020). Trends in Distributional Characteristics: Existence of Global Warming. *Journal of Econometrics 214*(1), 153–174.

Gadea, M. D. and J. Gonzalo (2025). Climate Change Heterogeneity: A New Quantitative Approach. *PloS one 20*(1), e0317208.

Gilli, M., M. Calcaterra, J. Emmerling, and F. Granella (2024). Climate Change Impacts on the Within-country Income Distributions. *Journal of Environmental Economics and Management 127*, 103012.

Giraldo, C., I. Giraldo, J. E. Gomez-Gonzalez, and J. M. Uribe (2025). Climate Growth at Risk in the Global South. *Energy Economics 149*, 108790.

Gonçalves, S., A. M. Herrera, L. Kilian, and E. Pesavento (2024). State-dependent Local Projections. *Journal of Econometrics 244*(2), 105702.

Hamilton, J. D. (2018). Why You Should Never Use the Hodrick-Prescott Filter. *Review of Economics and Statistics 100*(5), 831–843.

Hansen, J., L. Nazarenko, R. Ruedy, M. Sato, J. Willis, A. Del Genio, D. Koch, A. Lacis, K. Lo, S. Menon, et al. (2005). Earth's Energy Imbalance: Confirmation and Implications. *science 308*(5727), 1431–1435.

Harris, I., T. J. Osborn, P. Jones, and D. Lister (2020). Version 4 of the CRU TS Monthly High-resolution Gridded Multivariate Climate Dataset. *Scientific data 7*(1), 109.

Hassler, J., P. Krusell, and C. Olovsson (2024). The Macroeconomics of Climate Change: Starting Points, Tentative Results, and a Way Forward. *The Green Frontier: Assessing the Economic Implications of Climate Action*, 53.

Hsiang, S. (2016). Climate Econometrics. *Annual Review of Resource Economics 8*(1), 43–75.

Hsiang, S., R. Kopp, A. Jina, J. Rising, M. Delgado, S. Mohan, D. J. Rasmussen, R. Muir-Wood, P. Wilson, M. Oppenheimer, et al. (2017). Estimating Economic Damage from Climate Change in the United States. *Science 356*(6345), 1362–1369.

Ji, F., Z. Wu, J. Huang, and E. Chassignet (2014). Evolution of Land Surface Air Temperature Trend. *Nature Climate Change 4*, 462–466.

Jordà, Ò. (2005). Estimation and Inference of Impulse Responses by Local Projections. *American economic review 95*(1), 161–182.

Jordà, Ò. and A. M. Taylor (2024, August). Local Projections. NBER Working Papers 32822, National Bureau of Economic Research, Inc.

Kahn, M. E., K. Mohaddes, R. N. Ng, M. H. Pesaran, M. Raissi, and J.-C. Yang (2021). Long-term Macroeconomic Effects of Climate Change: A Cross-country Analysis. *Energy Economics 104*, 105624.

Kim, H. S., C. Matthes, and T. Phan (2025). Severe Weather and the Macroeconomy. *American Economic Journal: Macroeconomics 17*(2), 315–341.

Knutti, R. and M. A. Rugenstein (2015). Feedbacks, Climate Sensitivity and the Limits of Linear Models. *Philosophical Transactions of the Royal Society A: Mathematical, Physical and Engineering Sciences 373*(2054), 20150146.

Kopits, E., D. Kraynak, B. Parthum, L. Rennels, D. Smith, E. Spink, J. Perla, and N. Burns (2025). Economic Impacts of Climate Change in the United States: Integrating and Harmonizing Evidence from Recent Studies. *arXiv preprint arXiv:2509.00212*.

Kotz, M., F. Kuik, E. Lis, and C. Nickel (2024). Global Warming and Heat Extremes to Enhance Inflationary Pressures. *Communications Earth & Environment 5*(1), 116.

Kotz, M., L. Wenz, A. Stechemesser, M. Kalkuhl, and A. Levermann (2021). Day-to-day Temperature Variability Reduces Economic Growth. *Nature Climate Change 11*(4), 319–325.

Lemoine, D., C. Hausman, and J. G. Shrader (2025). A Guide to Climate Damages. Technical report, National Bureau of Economic Research.

Lucidi, F. S., M. M. Pisa, and M. Tancioni (2024). The Effects of Temperature Shocks on Energy Prices and Inflation in the Euro Area. *European Economic Review 166*, 104771.

Mumtaz, H. and A. Theophilopoulou (2024). The Distributional Effects of Climate Change. An Empirical Analysis. *European Economic Review 169*, 104828.

Nath, I. B., V. A. Ramey, and P. J. Klenow (2024, July). How Much Will Global Warming Cool Global Growth? Working Paper 32761, National Bureau of Economic Research.

Neal, T. (2023, June). The Importance of External Weather Effects in Projecting the Economic Impacts of Climate Change. Discussion Papers 2023-09, School of Economics, The University of New South Wales.

Newell, R. G., B. C. Prest, and S. E. Sexton (2021). The GDP-temperature Relationship: Implications for Climate Change Damages. *Journal of Environmental Economics and Management 108*, 102445.

Nguyen, H. M. (2024). Beyond the Annual Averages: Impact of Seasonal Temperature on Employment Growth in US Counties. *Journal of Environmental Economics and Management 125*, 102946.

Nordhaus, W. D. (1992). An Optimal Transition Path for Controlling Greenhouse Gases. *Science 258*(5086), 1315–1319.

Pintus, F. J., J. Jacobs, and S. Elmer (2024, Dec). Fiscal Impacts of Climate Anomalies. CESifo Working Paper Series 11548, CESifo.

Quesada, B., R. Vautard, P. Yiou, M. Hirschi, and S. I. Seneviratne (2012). Asymmetric European Summer Heat Predictability from Wet and Dry Southern Winters and Springs. *Nature Climate Change 2*(10), 736–741.

Screen, J. A. and I. Simmonds (2014). Amplified Mid-latitude Planetary Waves Favour Particular Regional Weather Extremes. *Nature Climate Change 4*(8), 704–709.

Seneviratne, S. I., X. Zhang, M. Adnan, W. Badi, C. Dereczynski, A. D. Luca, S. Ghosh, I. Iskandar, J. Kossin, S. Lewis, et al. (2021). *Weather and Climate Extreme Events in a Changing Climate*. Cambridge University Press.

Stock, J. H. and M. W. Watson (2016). Dynamic Factor Models, Factor-Augmented Vector Autoregressions, and Structural Vector Autoregressions in Macroeconomics. In *Handbook of macroeconomics*, Volume 2, pp. 415–525. Elsevier.

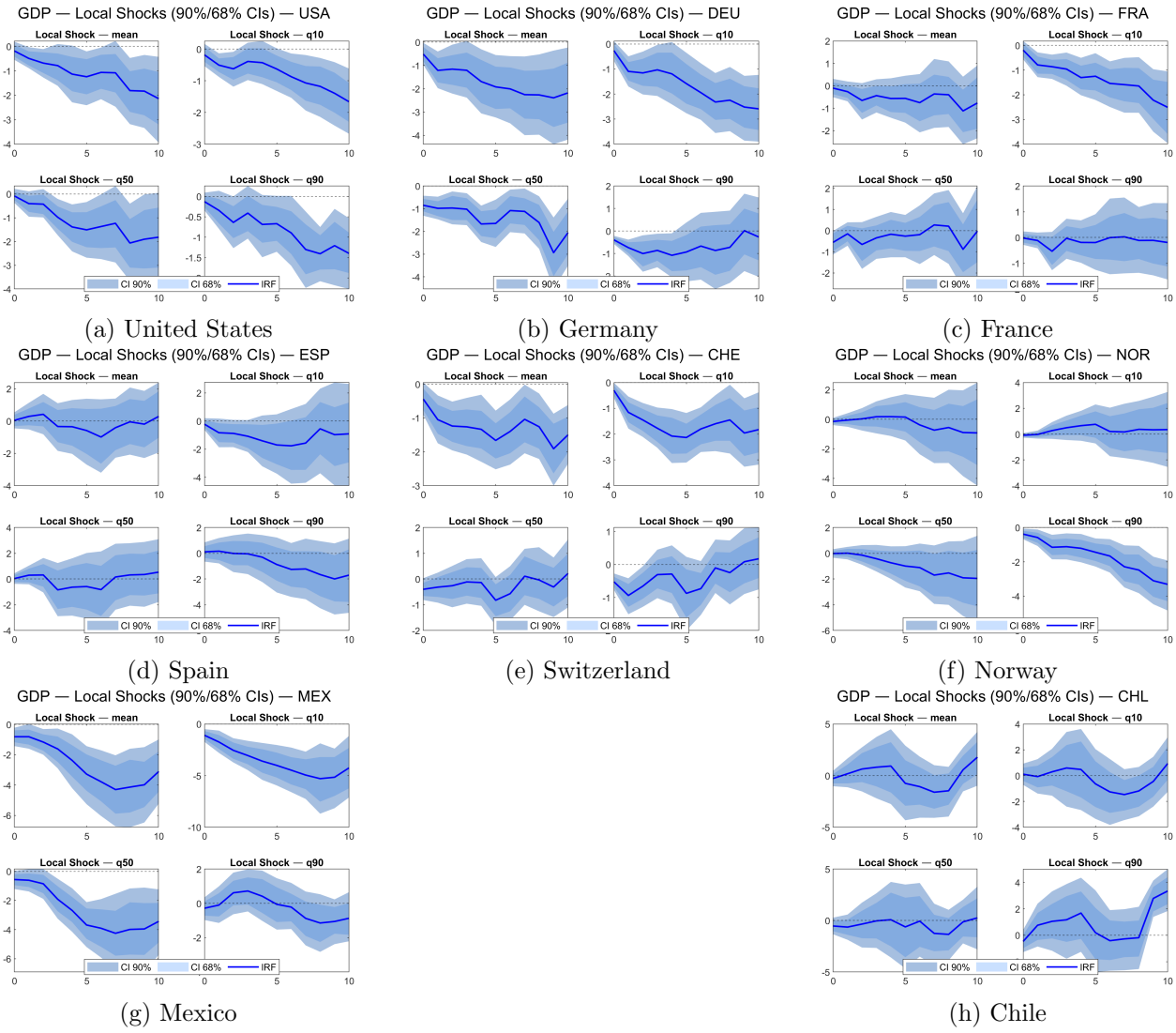
Tol, R. (2002). Estimates of the Damage Costs of Climate Change. Part 1: Benchmark Estimates. *Environmental and Resource Economics 21*, 47–73.

Trenberth, K. E., J. T. Fasullo, and M. A. Balmaseda (2014). Earth's Energy Imbalance. *Journal of Climate 27*(9), 3129–3144.

Zenios, S. A. (2022). The Risks from Climate Change to Sovereign Debt. *Climatic Change 172*(3), 30.

A Appendix

A.1 Supplementary Figures

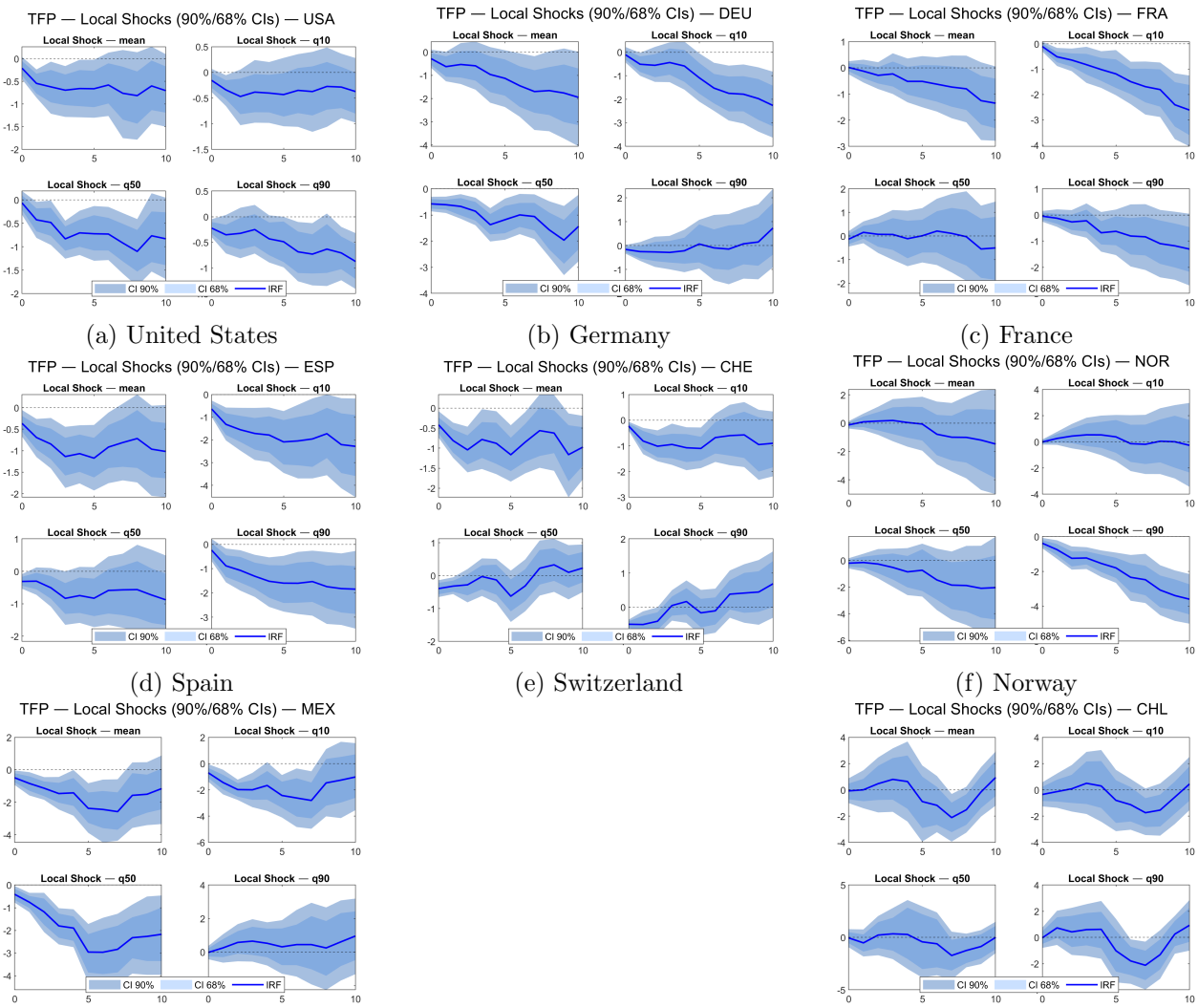


(a) United States (b) Germany (c) France

(d) Spain (e) Switzerland (f) Norway

(g) Mexico (h) Chile

Figure A1: GDP per-capita growth responses to individual local temperature distributional shocks

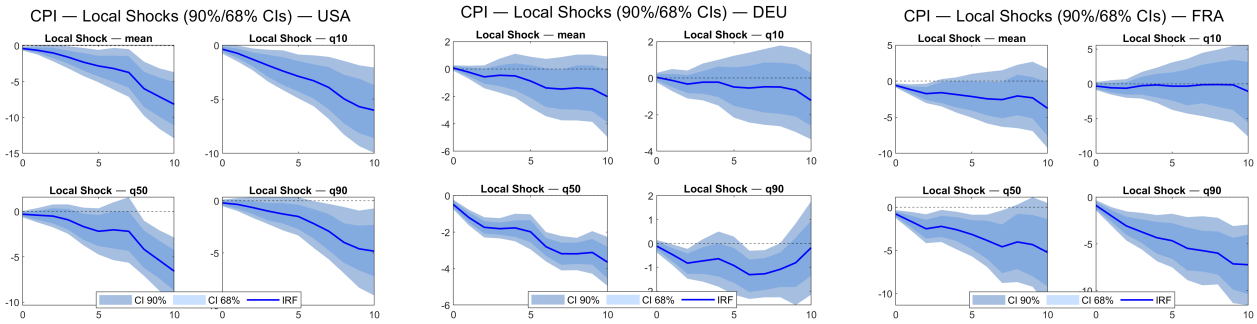


(a) United States (b) Germany (c) France

(d) Spain (e) Switzerland (f) Norway

(g) Mexico (h) Chile

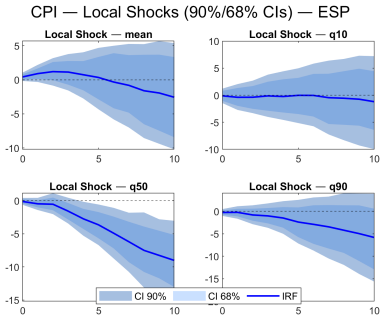
Figure A2: TFP growth responses to individual local temperature distributional shocks



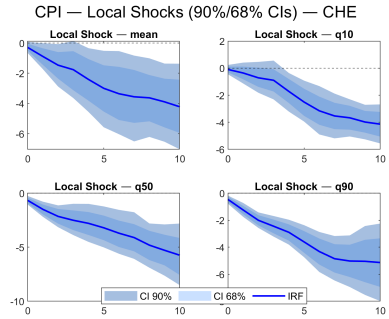
(a) United States

(b) Germany

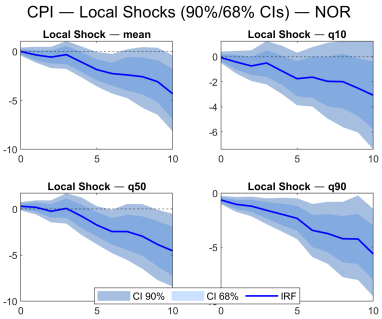
(c) France



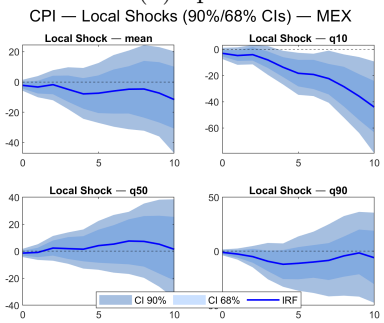
(d) Spain



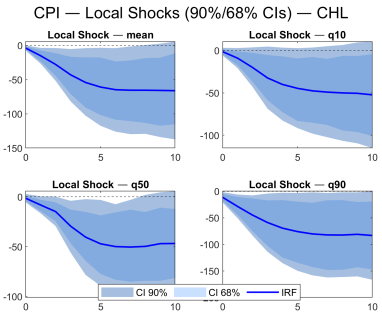
(e) Switzerland



(f) Norway

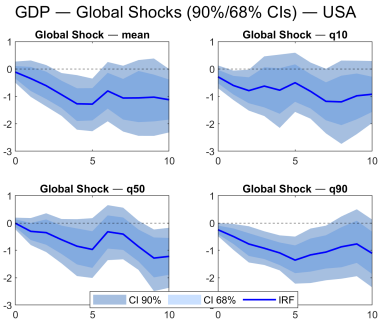


(g) Mexico

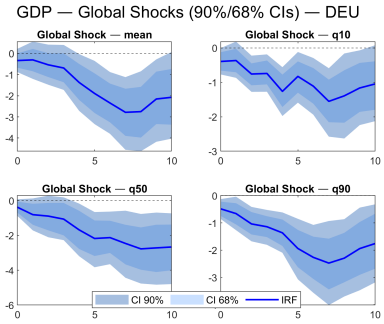


(h) Chile

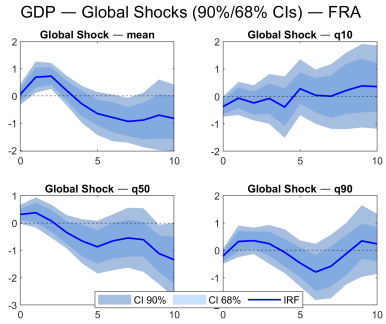
Figure A3: Prices responses to individual local temperature distributional shocks



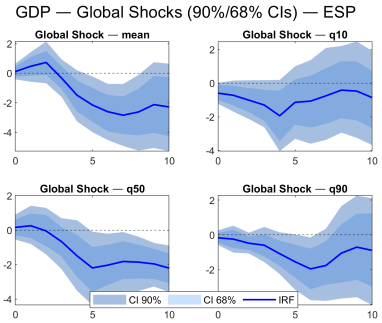
(a) United States



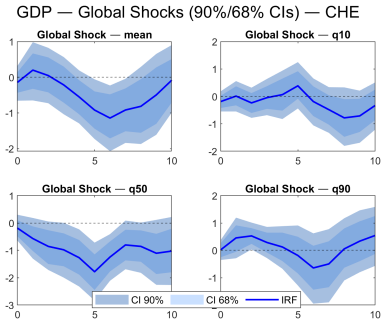
(b) Germany



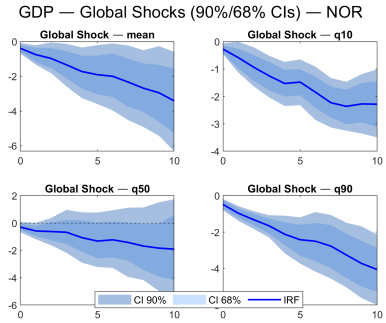
(c) France



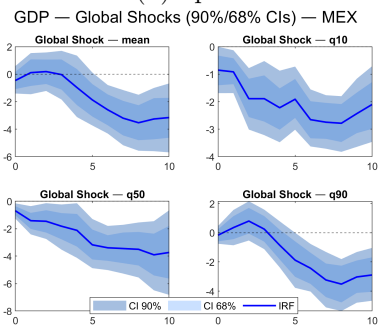
(d) Spain



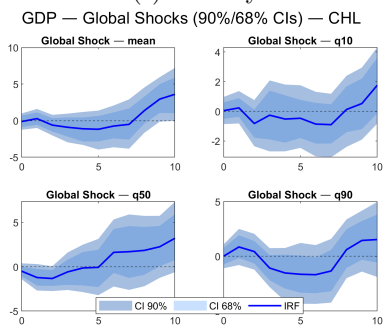
(e) Switzerland



(f) Norway

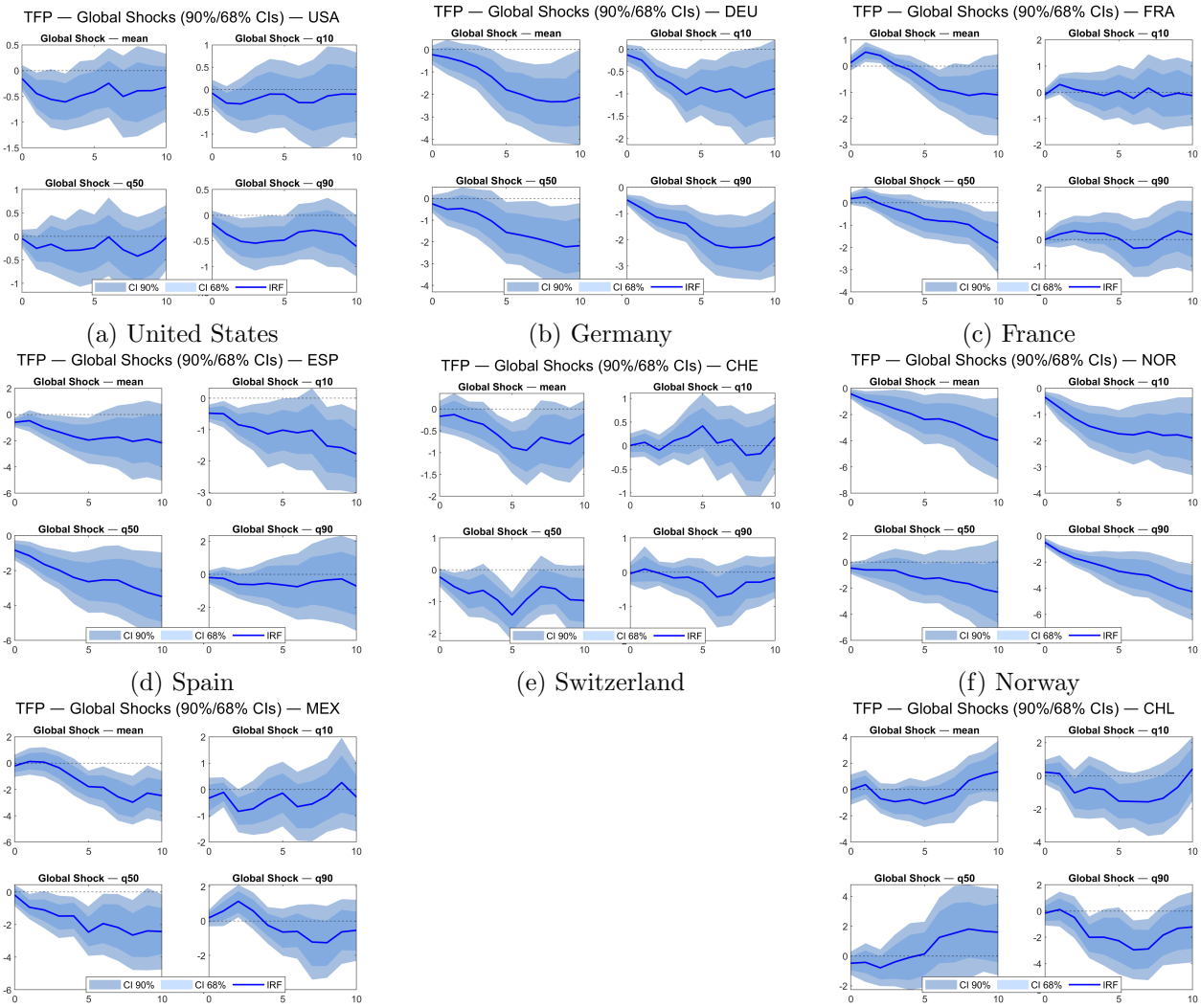


(g) Mexico



(h) Chile

Figure A4: GDP per-capita growth responses to individual global shocks

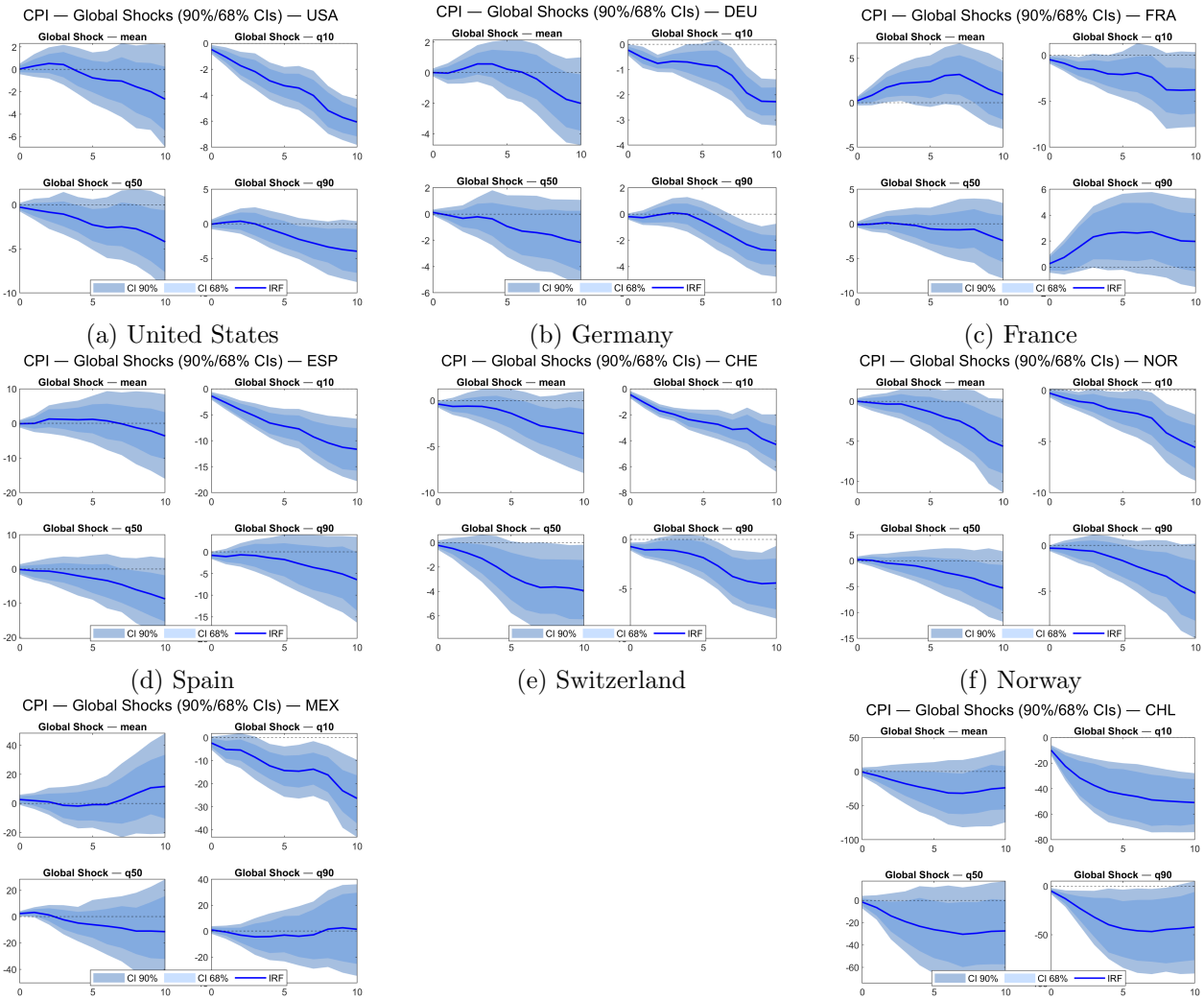


(a) United States (b) Germany (c) France

(d) Spain (e) Switzerland (f) Norway

(g) Mexico (h) Chile

Figure A5: TFP growth responses to individual global shocks



(a) United States (b) Germany (c) France

(d) Spain (e) Switzerland (f) Norway

(g) Mexico (h) Chile

Figure A6: Prices responses to individual global shocks

A.2 Supplementary Tables

Table A1: Joint and Sum Wald tests for GDP growth regressions

	Joint-test						Sum-test						
	Global			Local				Global			Local		
Country	F1	F2	F3	F1	F2	F3	Country	F1	F2	F3	F1	F2	F3
AUS	0.000	0.917	0.241	0.000	0.191	0.990	AUS	0.000	0.118	0.102	0.000	0.007	0.791
AUT	0.020	0.997	0.953	0.000	0.000	0.987	AUT	0.000	0.194	0.178	0.000	0.000	0.353
BEL	0.155	0.333	0.266	0.000	0.049	0.000	BEL	0.002	0.003	0.000	0.000	0.000	0.000
CAN	0.000	0.474	1.000	0.000	1.000	0.001	CAN	0.000	0.018	0.563	0.000	0.728	0.000
CHE	0.327	0.000	0.084	0.000	0.000	0.000	CHE	0.001	0.000	0.001	0.000	0.000	0.000
CHL	0.606	0.384	0.814	0.984	0.894	0.941	CHL	0.210	0.191	0.684	0.989	0.064	0.305
DEU	0.000	1.000	0.993	0.000	0.062	0.002	DEU	0.000	0.732	0.212	0.000	0.000	0.000
DNK	0.000	0.954	0.000	0.031	0.818	0.085	DNK	0.000	0.253	0.000	0.000	0.631	0.040
ESP	0.000	0.003	0.837	0.968	0.995	0.000	ESP	0.000	0.000	0.545	0.082	0.852	0.000
FIN	0.000	0.000	0.913	0.000	0.069	0.113	FIN	0.000	0.000	0.784	0.000	0.091	0.000
FRA	0.077	0.855	0.000	0.023	0.000	0.000	FRA	0.003	0.044	0.000	0.000	0.000	0.000
GBR	0.000	0.995	0.971	0.000	0.193	0.964	GBR	0.000	0.227	0.397	0.000	0.001	0.375
GRC	0.002	0.186	0.967	0.026	0.325	0.004	GRC	0.000	0.001	0.047	0.000	0.038	0.000
IRL	0.142	0.372	0.108	0.563	0.008	0.965	IRL	0.597	0.015	0.001	0.046	0.000	0.689
ITA	0.025	0.211	0.000	0.000	0.270	0.852	ITA	0.000	0.002	0.000	0.000	0.001	0.130
JPN	0.139	0.865	0.734	0.000	0.681	0.843	JPN	0.000	0.056	0.018	0.000	0.021	0.599
MEX	0.000	0.137	0.965	0.000	0.000	0.939	MEX	0.000	0.349	0.601	0.000	0.000	0.812
NOR	0.000	0.267	0.005	0.997	0.000	0.996	NOR	0.000	0.001	0.000	0.271	0.000	0.619
PRT	0.000	0.681	0.986	0.371	1.000	0.001	PRT	0.000	0.145	0.162	0.001	0.951	0.000
SWE	0.543	0.002	0.957	0.009	0.000	0.642	SWE	0.017	0.000	0.680	0.000	0.000	0.915
USA	0.000	0.975	0.339	0.000	1.000	0.844	USA	0.000	0.371	0.010	0.000	0.504	0.928

Notes: Each cell reports the p-values from Wald-type joint and sum significance tests applied to the local-projection impulse responses of cumulative GDP growth. The shock variables are the three identified temperature factors: F1 (*distributional shift*), F2 (*variability*), and F3 (*extremes*). Red and blue panels correspond to specifications under which the null hypothesis is rejected, indicating statistical significance.

Table A2: Joint and Sum Wald tests for TFP growth regressions

	Joint-test						**Sum-test**						
	Global			**Local**				**Global**			**Local**		
Country	F1	F2	F3	F1	F2	F3	Country	F1	F2	F3	F1	F2	F3
AUS	0.117	0.227	0.488	0.000	0.727	0.987	AUS	0.000	0.000	0.404	0.000	0.083	0.983
AUT	0.000	0.998	0.968	0.100	0.000	0.951	AUT	0.000	0.530	0.142	0.000	0.000	0.134
BEL	0.031	0.036	0.388	0.000	0.776	0.004	BEL	0.000	0.000	0.001	0.000	0.020	0.000
CAN	0.000	0.569	0.997	0.085	0.401	0.028	CAN	0.000	0.005	0.569	0.000	0.031	0.001
CHE	0.011	0.790	0.012	0.000	0.000	0.046	CHE	0.000	0.279	0.000	0.000	0.000	0.001
CHL	0.979	0.165	0.330	0.892	0.975	0.960	CHL	0.386	0.002	0.008	0.402	0.207	0.430
DEU	0.000	0.468	1.000	0.000	0.027	0.000	DEU	0.000	0.004	0.968	0.000	0.000	0.000
DNK	0.000	0.917	0.119	0.004	0.987	0.192	DNK	0.000	0.079	0.000	0.000	0.157	0.066
ESP	0.000	0.000	1.000	0.000	0.999	0.000	ESP	0.000	0.000	0.418	0.000	0.248	0.000
FIN	0.000	0.010	0.988	0.000	0.136	0.004	FIN	0.000	0.001	0.252	0.000	0.001	0.000
FRA	0.146	0.051	0.001	0.001	0.069	0.000	FRA	0.002	0.000	0.000	0.000	0.000	0.000
GBR	0.000	0.542	0.922	0.000	0.074	0.857	GBR	0.000	0.024	0.083	0.000	0.000	0.201
GRC	0.000	0.036	0.994	0.001	0.130	0.006	GRC	0.000	0.000	0.118	0.000	0.033	0.000
IRL	0.004	0.491	0.737	0.990	0.761	0.376	IRL	0.000	0.016	0.026	0.505	0.118	0.735
ITA	0.000	0.980	0.830	0.000	0.139	1.000	ITA	0.000	0.733	0.066	0.000	0.005	0.501
JPN	0.134	0.812	0.934	0.000	0.000	0.796	JPN	0.001	0.013	0.889	0.000	0.000	0.504
MEX	0.103	0.302	0.053	0.001	0.003	0.037	MEX	0.000	0.596	0.000	0.000	0.000	0.000
NOR	0.000	0.024	0.011	0.979	0.000	1.000	NOR	0.000	0.000	0.000	0.110	0.000	0.859
PRT	0.000	0.671	0.416	0.000	0.996	0.033	PRT	0.000	0.387	0.007	0.000	0.233	0.000
SWE	0.638	0.955	0.991	0.819	0.123	0.066	SWE	0.007	0.463	0.490	0.032	0.116	0.000
USA	0.003	0.622	0.999	0.000	0.666	0.700	USA	0.000	0.014	0.516	0.000	0.011	0.052

Notes: Each cell reports the p-values from Wald-type joint and sum significance tests applied to the local-projection impulse responses of cumulative TFP growth. The shock variables are the three identified temperature factors: F1 (*distributional shift*), F2 (*variability*), and F3 (*extremes*). Red and blue panels correspond to specifications under which the null hypothesis is rejected, indicating statistical significance.